POLITECNICO DI MILANO

School of Industrial and Information Engineering

Master of Science in Electrical Engineering

A New Empirical BESS Model for Primary Control Reserve

Supervisor: Prof. Marco Merlo

Candidate:
Hamid Malmir
Matr. 877251

Academic Year 2018-2019

To my parents Hassan Malmir and Shahrzad Eskandaripour, for giving birth to me in the first place and supporting me spiritually throughout my life, and to my family who always push me forward!

Acknowledgement

Foremost, I would like to express my sincere gratitude to my advisor Prof. Marco Merlo for his continuous support, patience, motivation, enthusiasm, and immense knowledge. His guidance helped me in all the time of research and writing of this thesis. I could not have imagined having a better advisor and mentor for my thesis.

Besides my advisor, I would like to thank Dr. Giuliano Rancilio for his friendliness, insightful comments, and continuous helps. I wish him the best luck with his future career.

Last but not the least, I would like to thank my friends, Marzieh Hosseini, Miad Ahmadi, Mahdi Bayat, Salman Oukati, Payam Norouzi, Leila Esfandiari, and Asal Tabaei.

Table of content

List of Figures

List of Tables

Abstract

Nowadays, with the fast growth of the grid penetration levels of renewable sources, guaranteeing the stability of the grid is becoming more and more difficult than it was in the past. Battery Energy Storage Systems (BESSs) are the most promising solutions for ancillary services provision among which Primary Control Reserve (PCR). Currently, the fastest BESS model is empirical model. Unfortunately, they are not enough accurate in State of Charge (SOC) estimation so that they are only used for the sizing of the battery pack but not the real time SOC monitoring. In this study, the development of an empirical BESS model for SOC estimation based on an experimental data of a Li-ion battery pack is proposed. The aim of this work is to develop a novel empirical model with high accuracy in SOC estimation.

Keywords: Empirical BESS model; battery energy storage system; ancillary services; primary control reserve;

Sommario

Oggi, con la rapida crescita dei livelli di penetrazione della rete da fonti rinnovabili, garantire la stabilità della rete sta diventando sempre più difficile di quanto non fosse in passato. I sistemi di accumulo dell'energia della batteria (BESSs) sono le soluzioni più promettenti per la fornitura di servizi ausiliari, tra cui la Riserva di controllo primario (PCR). Attualmente, il modello BESS più veloce è il modello empirico. Sfortunatamente, non sono abbastanza precisi nella stima dello stato di carica (SOC) in modo da essere utilizzati solo per il dimensionamento del pacco batteria ma non per il monitoraggio SOC in tempo reale. In questo studio, viene proposto lo sviluppo di un modello empirico BESS per la stima SOC basato su dati sperimentali di un pacco batterie agli ioni di litio. Lo scopo di questo lavoro è di sviluppare un nuovo modello empirico con elevata precisione nella stima SOC.

Parole chiave: modello empirico BESS; sistema di accumulo dell'energia della batteria; servizi ausiliari; riserva di controllo primaria;

Chapter 1

Introduction

The total renewable energy production is doubled by nine years from 2009 to 2018 [1]. As variable renewables grow to substantial levels, electricity systems will require greater flexibility. Unfortunately, most of the Renewable Energy Sources (RESs) are not programmable, so their generated power needs to be stored. Battery energy storage systems (BESSs) are a promising solution for this problem due to their inherent distributed features, their ability to inject and absorb power, their high-power ramping and ability to provide a set of different grid services. As of today, BESSs are being deployed to provide several different services, such as peak shaving [2], energy management of microgrids [3] and stochastic resources [4], [5] and frequency and voltage regulation [6], [7], [8]. By providing these essential services, electricity storage can drive serious electricity decarbonization and help transform the whole energy sector [9]. The Figure 1.1 and Figure 1.2 show Global electricity production in 2050.

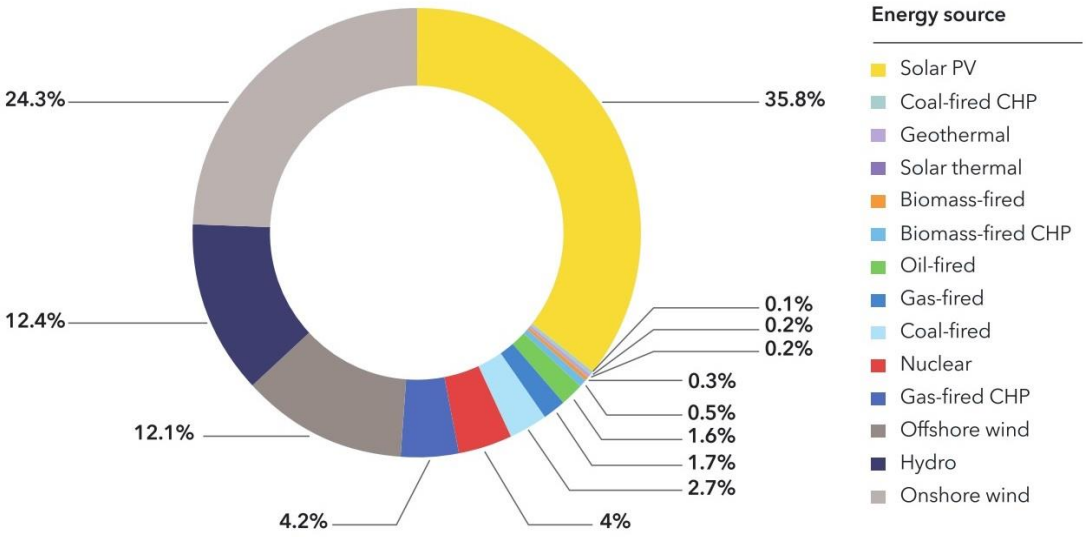

Figure 1.1 Global electricity production in 2050 [10]

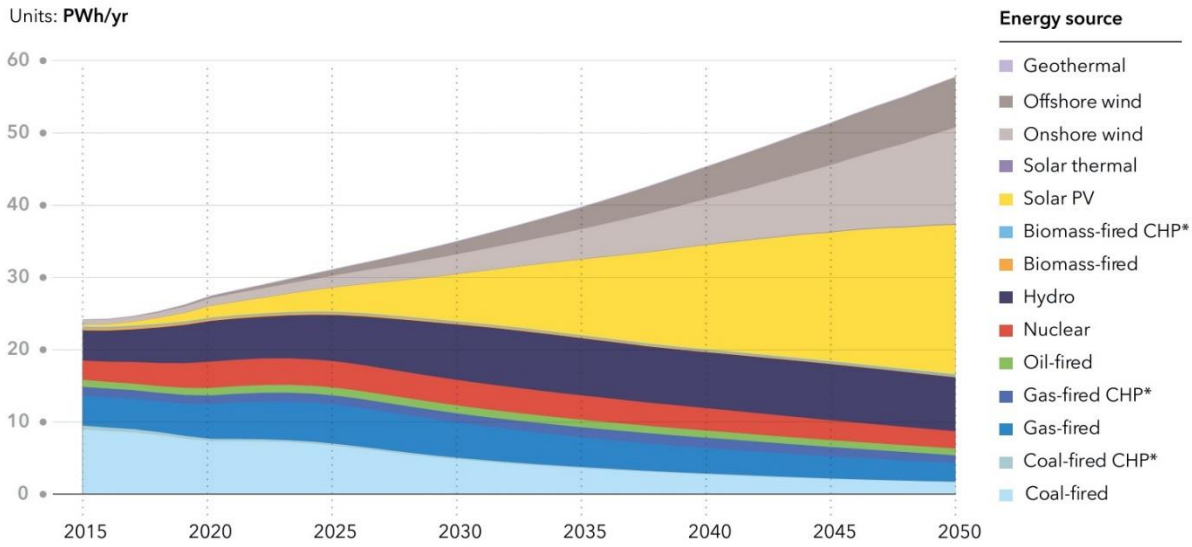

Figure 1.2 Global electricity production by generation type [10].

Recent technology advancement in battery storage in general has been intensified by high demand for batteries in electronic devices. Structural elements indicate not only that continued cost reductions are likely, but also that they are strongly linked to developments underway in the different sectors, for example, changes in battery characteristics (chemistry, energy density and size of the battery packs) and the scale of manufacturing plants. Today most battery production is in plants that range from 3 to 8 gigawatt-hours per year

(GWh/year) though three plants with over 20 GWh/year capacity are already in operation and five more are expected by 2023.

It is expected that by 2025 batteries will increasingly use cathode chemistries that are less dependent on cobalt, such as NMC 811,3 NMC 622 or NMC 532 cathodes in the NMC family or advanced NCA batteries. This will cause to an increase in energy density and a decrease of battery costs, in combination with other developments (e.g. the availability of silicon-graphite chemistries for anode technology). In the European Union, the Strategic Action Plan for Batteries in Europe was adopted in May 2018. It brings together a set of measures to support national, regional and industrial efforts to build a battery value chain in Europe, including raw material extraction, sourcing and processing, battery materials, cell production, battery systems, as well as reuse and recycling. In combination with the leverage offered by its market size, it seeks to attract investment and establish Europe as a player in the battery industry [11].

Stationary electricity storage can provide wide variety of energy services in an affordable manner. As the cost of emerging technologies decreases further, storage will become increasingly competitive, and the range of economical services it can provide will increase [9].

The structure of the thesis is outlined in the following. In Chapter 2, an introduction on the different types of energy storage technology and SOC models is given. In chapter 3, Ancillary Services Market is explained. Chapter 4 is about methodology that is used for modeling of the empirical model. The simulations performed with the model presented in Chapter 5 are presented, and in the chapter 6, the conclusion of the model and the simulations results are given.

Chapter 2

Energy Storage Systems

The main goal of this chapter is to give a background about energy storage systems, battery parameters, and short review of different battery models. There are several methods to store energy. With advancing the technologies, the number of equipment that can store energy in different ways are increasing. In the following, some of the most popular technology of storing energy is explained.

2.1 Different Energy Storage Technologies

2.1.1 Ultracapacitors

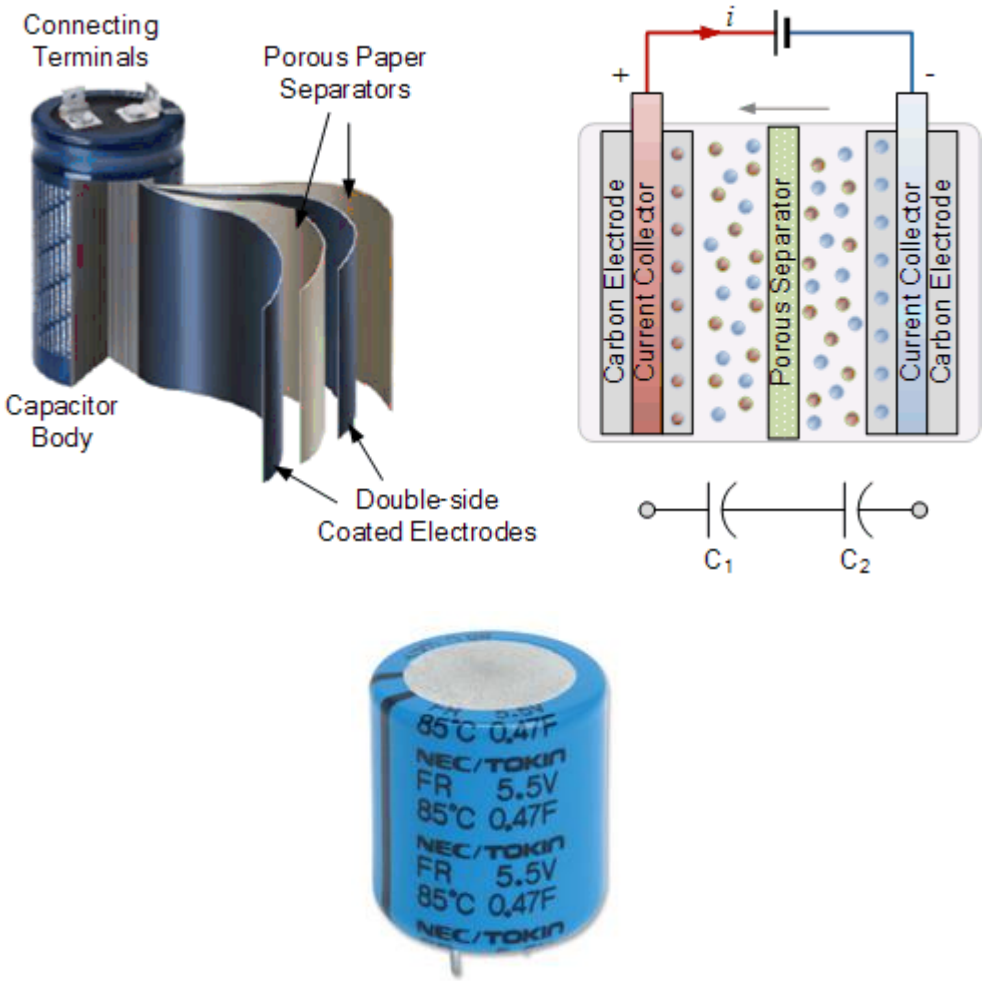

Figure 2.1 Ultracapcitor [12]

An ultracapacitor is an electrochemical device consisting of two porous electrodes, usually made up of activated carbon immersed in an electrolyte solution that stores charge electrostatically. This arrangement effectively creates two capacitors, one at each carbon electrode, connected in series. The ultracapacitor is available with capacitances in the hundreds of farads all within a very small physical size and can achieve much higher power density than batteries. However, the voltage rating of an ultracapacitor is usually less than

about 3 volts so several capacitors have to be connected in series and parallel combinations to provide any useful voltage.

Ultracapacitors can be used as energy storage devices similar to a battery, and in fact are classed as an ultracapacitor battery. But unlike a battery, they can achieve much higher power densities for a short duration. They are used in many hybrid petrol vehicles and fuel cell driven electric vehicles because of their ability to quickly discharge high voltages and then be recharged. But by operating ultracapacitors with fuel cells and batteries peak power demands, and transient load changes can be controlled more efficiently [12].

2.1.2 Flywheels

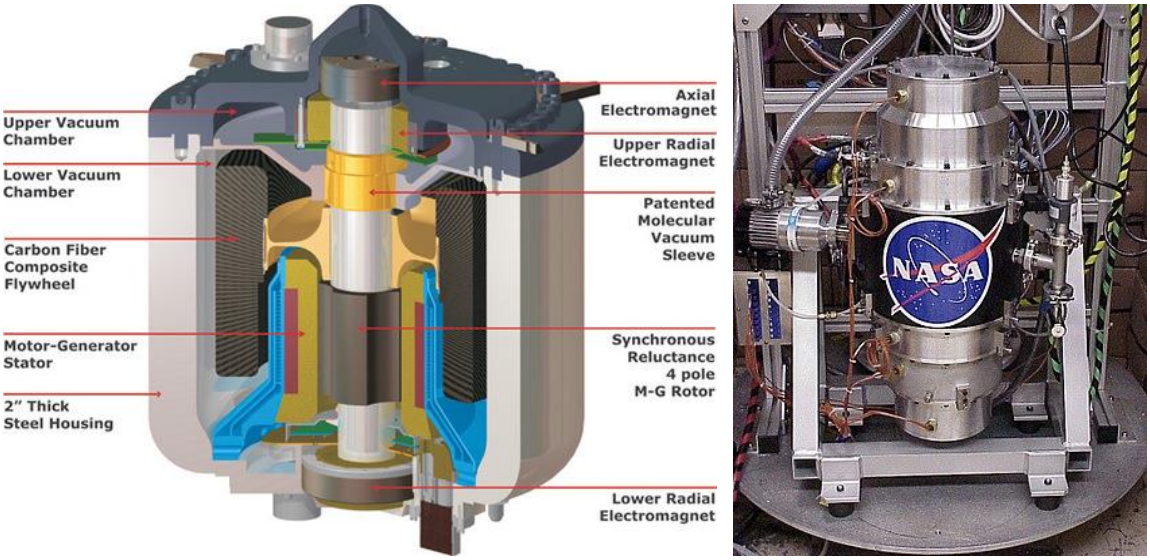

Figure 2.2 Freewheel Layout [13], [14]

A flywheel is a mechanical device specifically designed to convert electrical energy to kinetic energy (rotational energy). Flywheels resist changes in rotational speed by their moment of inertia. The amount of energy stored in a flywheel is proportional to the square of its rotational speed and its mass. The way to change a flywheel's stored energy without changing its mass is by increasing or decreasing its rotational speed. Since flywheels act as

mechanical energy storage devices, they are the kinetic-energy-storage analogue to electrical inductors, for example, which are a type of accumulator.

Flywheels are typically made of steel and rotate on conventional bearings; these are generally limited to a maximum revolution rate of a few thousand RPM [15]. High energy density flywheels can be made of carbon fiber composites and employ magnetic bearings, enabling them to revolve at speeds up to 60,000 RPM (1 kHz) [16]. Carbon-composite flywheel batteries have recently been manufactured and are proving to be viable in real-world tests on mainstream cars. Additionally, their disposal is more eco-friendly than traditional lithium ion batteries [17].

2.1.3 Fuel cells

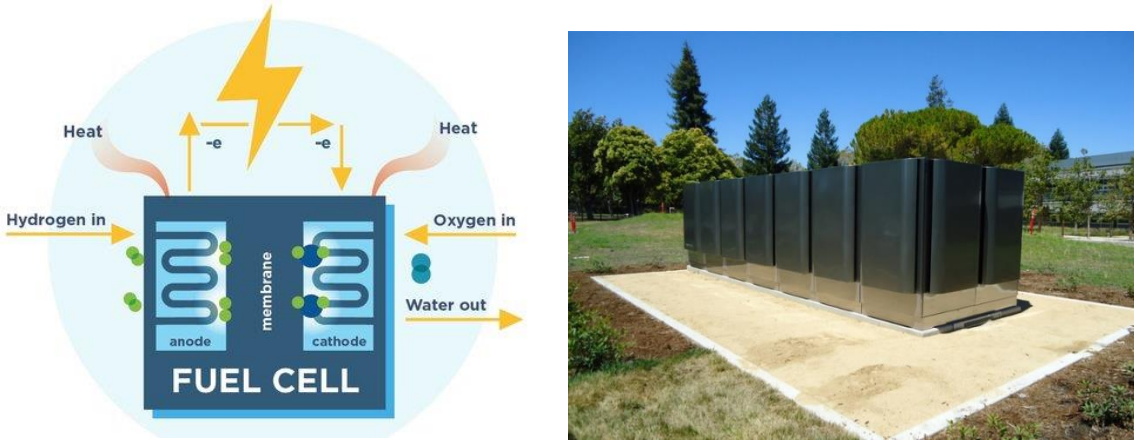

Figure 2.3 Fuel cell structure and stationary application [18].

Unlike traditional combustion technologies that burn fuel, fuel cells undergo a chemical process to convert hydrogen-rich fuel into electricity. Fuel cells do not need to be periodically recharged like batteries, but instead continue to produce electricity as long as a fuel source is provided [18].

A fuel cell is composed of an anode, a cathode, and an electrolyte membrane. A fuel cell works by passing hydrogen through the anode of a fuel cell and oxygen through the

cathode. At the anode site, the hydrogen molecules are split into electrons and protons. The protons pass through the electrolyte membrane, while the electrons are forced through a circuit, generating an electric current and excess heat. At the cathode, the protons, electrons, and oxygen combine to produce water molecules. Due to their high efficiency, fuel cells are very clean, with their only by-products being electricity, excess heat, and water. In addition, as fuel cells do not have any moving parts, they operate near-silently [18].

Advantages at a glance:

- Low-to-Zero Emissions
- High Efficiency
- Reliability
- Fuel Flexibility
- Energy Security
- Durability
- Scalability
- Quiet Operation

Disadvantages at a glance:

- Average efficiency (lower w.r.t batteries, even lower if you consider the efficiency of the electrolyzer, too)
- low specific power
- Expensive to manufacture due the high cost of catalysts (platinum)
- Lack of infrastructure to support the distribution of hydrogen
- A lot of the currently available fuel cell technology is in the prototype stage and not yet validated
- Hydrogen is expensive to produce and not widely available

2.1.4 Batteries

A battery is a device consisting of one or more electrochemical cells with external connections for powering electrical devices [19]. They are classified into two main groups:

2.1.4.1 Primary Batteries

Primary (single-use or "disposable") batteries are used once and discarded, as the electrode materials are irreversibly changed during discharge; a common example is the alkaline battery used for flashlights and a multitude of portable electronic devices [20]. In general, these have higher energy densities than rechargeable batteries [21]. Common types of disposable batteries include zinc–carbon batteries and alkaline batteries.

2.1.4.2 Secondary Batteries

Secondary (rechargeable) batteries can be discharged and recharged multiple times using an applied electric current; the original composition of the electrodes can be restored by reverse current. Examples include the lead-acid batteries used in vehicles and lithium-ion batteries used for portable electronics such as laptops and mobile phones [20].

2.1.4.3 Lithium Batteries

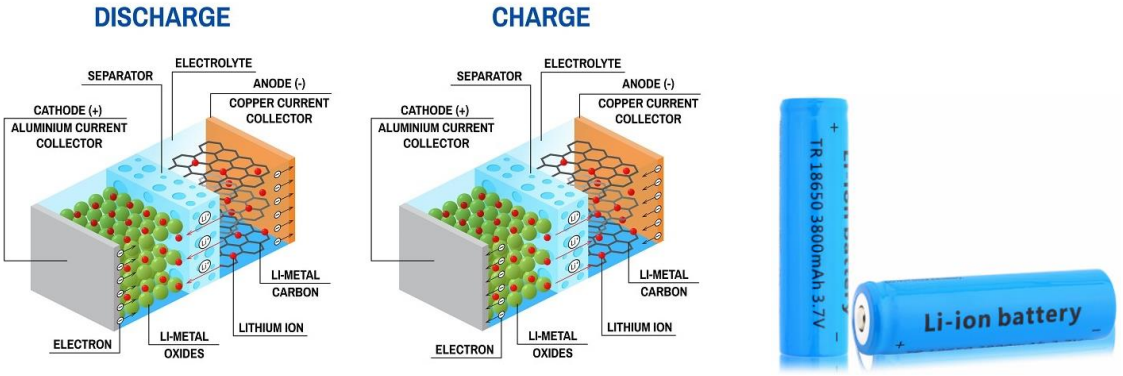

Figure 2.4 Lithium ion battery structure [22] and Lithium battery cell [23].

A lithium-ion battery or Li-ion battery (LIB) is a type of rechargeable battery. Lithium-ion batteries are commonly used for portable electronics and electric vehicles and are growing in popularity for military and aerospace applications [24]. The lithium ions within a lithium ion battery migrate back and forth between the two electrodes during charging and discharging. The ions travel between the anode and the cathode via a separator by an electrolyte commonly composed a lithium salt (e.g. LiPF6) in an organic solvent. The electrolyte solution plays a critical role within LIBs by enabling an effective conduction of the lithium ions between the electrodes. Additives are commonly added into the electrolyte solution to improve performance, enhance stability, prevent solution degradation and prevent dendritic lithium formation. The prevention of dendritic lithium formation is key to achieving battery safety as the lithium dendrites establish a connection between the electrodes, causing the battery to overheat and become a potential fire hazard. The electrolytes and their additives are commonly used in LIBs to identify the current density, stability and the reliability of the final battery. The properties of the electrolyte are therefore critical to the overall performance of the battery. Electrolytes must possess a good ionic conductivity and be electrically insulating, they should have a wide electrochemical window, they must be inert to other battery components and they must be chemically and thermally stable. In addition, electrolytes of a high purity (free from contamination) help to prevent oxidation at the electrode and promote a good cycle life [22].

This Lithium-ion Battery technology is popular because of the high energy density (high voltage combined with high specific capacity), high discharge rate, and high security and low cost [13].

Advantages at a glance:

- High specific energy and high load capabilities with Power Cells.
- Long cycle and extend shelf-life; maintenance-free.
- High capacity, low internal resistance, good coulombic efficiency.
- Simple charge algorithm and reasonably short charge times.
- Low self-discharge (less than half that of NiCd and NiMH).

Disadvantages at a glance:

- Requires protection circuit to prevent thermal runaway if stressed.
- Degrades at high temperature and when stored at high voltage.
- No rapid charge possible at freezing temperatures (<0°C, <32°F).
- Transportation regulations required when shipping in larger quantities.

2.1.4.4 Nickel Cadmium Batteries

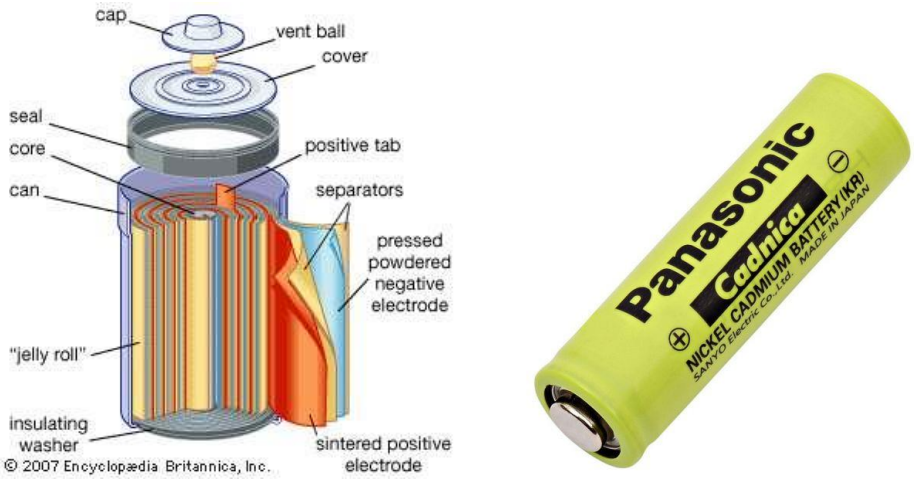

Figure 2.5 Nickel cadmium battery structure [25] and Nickel cadmium cell [26].

Invented by Waldemar Jungner in 1899, the nickel-cadmium battery offered several advantages over lead acid, then the only other rechargeable battery; however, the materials for NiCd were expensive [27]. The nickel cadmium battery consists of a nickel-positive electrode (cathode) and a cadmium-negative electrode (anode) in potassium hydroxide solution [28].

Developments were slow, but in 1932, advancements were made to deposit the active materials inside a porous nickel-plated electrode. Further improvements occurred in 1947 by absorbing the gases generated during charge, which led to the modern sealed NiCd battery. For many years, NiCd was the preferred battery choice for two-way radios, emergency medical equipment, professional video cameras and power tools. In the late 1980s, the ultra-high capacity NiCd rocked the world with capacities that were up to 60 percent higher than the standard NiCd. Packing more active material into the cell achieved this, but the gain was shadowed by higher internal resistance and reduced cycle count [27].

Advantages at a glance:

- Rugged, high cycle count with proper maintenance.
- Only battery that can be ultra-fast charged with little stress.
- Good load performance; forgiving if abused.
- Simple storage and transportation; not subject to regulatory control.
- Good low-temperature performance.
- Economically priced; NiCd is the lowest in terms of cost per cycle.

Disadvantages at a glance:

- Relatively low specific energy compared with newer systems.
- Memory effect; needs periodic full discharges and can be rejuvenated.
- Cadmium is a toxic metal. Cannot be disposed of in landfills.
- High self-discharge; needs recharging after storage.
- Low cell voltage of 1.20V requires many cells to achieve high voltage.

2.1.4.5 Lead Acid Batteries

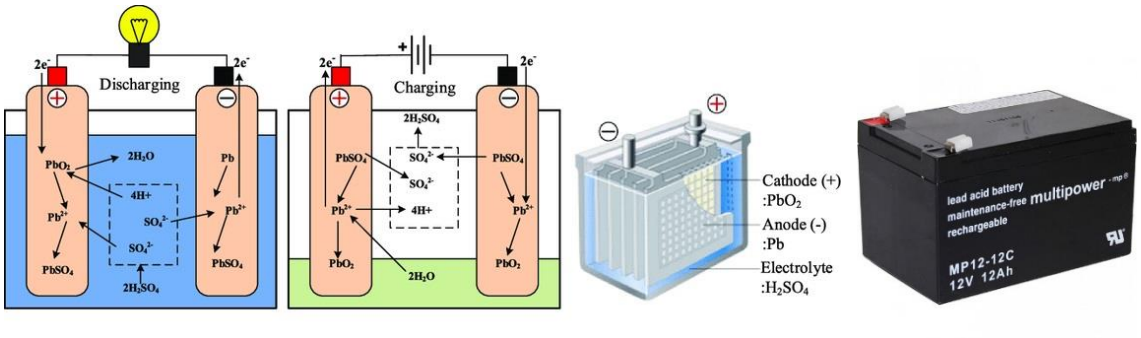

Figure 2.6 Lead acid battery structure [29], [30] and Sealed lead acid battery [31].

Invented by the French physician Gaston Planté in 1859, lead acid was the first rechargeable battery for commercial use. Lead acid batteries have been used as energy sources commercially since 1860 [32]. LA batteries are used in every internal combustion engine (ICE) vehicle as a starter and typically applied for uninterrupted power supply (UPS), renewable energy storage, and grid storage because of their ruggedness, safe operation, temperature tolerance, and low cost [33], [30]. The battery consists of Pb as negative electrode, PbO2 as positive electrode, and H2SO4 solution as electrolyte [29], [34]. Despite its advanced age, the lead chemistry continues to be in wide use today. There are good reasons for its popularity; lead acid is dependable and inexpensive on a cost-per-watt base. There are few other batteries that deliver bulk power as cheaply as lead acid, and this makes the battery cost-effective energy storage source.

The grid structure of the lead acid battery is made from a lead alloy. Pure lead is too soft and would not support itself, so small quantities of other metals are added to get the mechanical strength and improve electrical properties. The most common additives are antimony, calcium, tin and selenium. These batteries are often known as “Lead-antimony” and “Lead-calcium”. Adding antimony and tin improves deep cycling but this increases water consumption and escalates the need to equalize. Calcium reduces self-discharge, but the positive lead-calcium plate has the side effect of growing due to grid oxidation when being over-charged. Modern lead acid batteries also make use of doping agents such as selenium, cadmium, tin and arsenic to lower the antimony and calcium content [35].

Lead acid is heavy and is less durable than nickel and lithium-based systems when deep cycled. A full discharge causes strain and each discharge/charge cycle permanently robs the battery of a small amount of capacity. This loss is small while the battery is in good operating condition, but the fading increases once the performance drops to half the nominal capacity. This wear-down characteristic applies to all batteries in various degrees [35].

Advantages at a glance:

- Inexpensive and simple to manufacture; low cost per watt-hour.
- Low self-discharge; lowest among rechargeable batteries.
- High specific power, capable of high discharge currents.
- Good low and high temperature performance.

Disadvantages at a glance:

- Low specific energy; poor weight to energy ratio.
- Slow charge; fully saturated charge takes 14-16 hours.
- Must be stored in charged condition to prevent sulfating.
- Limited cycle life; repeated deep-cycling reduces battery life.
- Flooded version requires watering.
- Transportation restrictions on the flooded type.
- Not environmentally friendly.

2.2 Important parameters of a battery

During using a battery, it is important to consider some of the most important parameters of a battery in order to get the highest level of safety and quality. In the following some of these parameters are explained:

2.2.1 Ageing Mechanism and safe operation

Battery ageing, increasing cell impedance, power fading, and capacity fading origin from multiple and complex mechanisms. Although, the quantities that have highest effect on calendar ageing are storage temperature and SoC level [36]- [37], material parameters, as well as storage and cycling conditions, have an impact on battery life-time and performance. Due to ageing mechanisms such as Solid-Electrolyte Interphase (SEI) and positive electrode loss in conductivity, Power fading (or efficiency fading) occurs which is a consequence of internal resistances increment. Another degradation related to ageing is Capacity fading. Many mechanisms such as SEI formation [38] causes less room for Lithium storage or lithium consumption and decrement in energy exchange during each cycle. All these events lead to capacity fading. As capacity fading and power fading originate from a number of various processes and their interactions, these processes cannot be studied independently and occur at similar timescales, complicating the investigation of ageing mechanisms. Many of the mechanisms responsible for battery decay and ageing can be monitored and investigated non-destructively by the use of impedance spectroscopy. Although the interpretation of impedance data is challenging and not always clear. Impedance spectroscopy, together with the more conventional methods of battery science, electrochemical and other, is a powerful tool for the investigation of ageing processes in lithium-ion batteries [39], [40].

Depending on the cell chemistry, both high and low state of charge may deteriorate performance and shorten battery life. At high temperatures, the decay is accelerated, but low temperatures, especially during charging, also can have a negative impact. Amongst the material parameters, surface chemistry plays a major role for both anode and cathode materials. On the cathode, phase transitions and structural changes in the bulk material strongly influence ageing, while changes in the bulk anode material are considered of minor importance only. Unfortunately, lithium-ion batteries are complex systems to understand, and the processes of their ageing are even more complicated [39].

2.2.2 End of life

Battery End of Life is capacity fade which causes a decrement of the available capacity from 100% to 80% of nominal capacity of the battery. Generally speaking, end of life for a battery will be determined in one of three different ways depending on the product's manufacturer:

2.2.2.1 Cycle life

This refers to the total number of times that a battery can be charged and discharged. Manufacturers will typically include the recommended cycle life on the product's packaging or in other documentation available at the time of purchase.

2.2.2.2 Warrantied life

This will usually be outlined in a specific number of years, like any other product that you may have. A battery with a 12-year life under warranty is typically expected to reach true end of life by roughly that time.

2.2.2.3 Total energy throughput

This is the total amount of energy that will pass through the battery over the course of its lifespan and this will usually be measured in megawatt-hours.

2.2.3 Operational life

Occasionally, manufacturers will reference end of life using a measurement called operational life expected. If this is present, it will usually be somewhat longer than the "warrantied life" measurement. At that point, the battery will no longer be covered under

any type of manufacturer's warranty, but it will still continue to function until about the time that the listed number of years have passed.

2.2.4 State of health

SOH is a quantifying estimation that reflects the general condition of a battery and its ability to deliver the specified performance compared with a fresh battery. SOH monitoring in batteries has a wide variety of connotations, ranging from intermittent manual measurements of voltage and electrolyte parameters to fully automated online supervision of various measured and estimated battery parameters [41]. State of health can be defined as the ratio of the actual capacity and the nominal capacity of the battery:

$$SOH = 100 * \frac{C_{actual}}{C_n} \ [\%] \qquad (2.1)$$

2.2.5 Temperature

Lithium-ion battery performance is sensitive to temperature, while temperature uniformity and maximum temperature are important to thermal safety as well as aging. Thermal problems are possible if thermal safety measures are not taken, especially for charging with continuous high current. Therefore, lithium-ion batteries should be precisely checked and handled to avoid safety performance related problems [42]. A lot of efforts have been carried out to improve the charging performance from the view of charging algorithm and reaction mechanism analysis [43], [44].

2.2.6 C-rate and E-rate

A measure of the rate at which a battery can be charged or discharged is called the C-rate. It is defined as the current through the battery divided by the theoretical current draw

under which the battery would deliver its nominal rated capacity in one hour. For example, A 1C rate means that the discharge current will discharge the entire battery in 1 hour. For a battery with a capacity of 100 Amp-hours, this equates to a discharge current of 100 Amps. A 5C rate for this battery would be 500 Amps, and a C/2 rate would be 50 Amps. Similarly, an E-rate describes the discharge power. A 1E rate is the discharge power to discharge the entire battery in 1 hour [45].

$$C - rate = \frac{I}{C_n} \qquad [\frac{1}{h}] \tag{2.2}$$

Where I is the DC current in the interval, and C_n is the nominal capacity of the battery.

2.2.7 Cycles and efficiency

There are different ways to define a battery cycle. one definition is that a cycle is a process that takes a battery from an initial SoC value to an equal final SoC value [46]. Efficiency of a cycle can be computed as follows:

$$\eta = \frac{E_{dis}}{E_{ch}} * 100 \qquad [\%] \tag{2.3}$$

Where E_{dis} is the injected energy with a battery to the grid during discharge cycles, and E_{ch} is the absorbed energy from the grid during charge cycles.

2.3 Ragone Chart

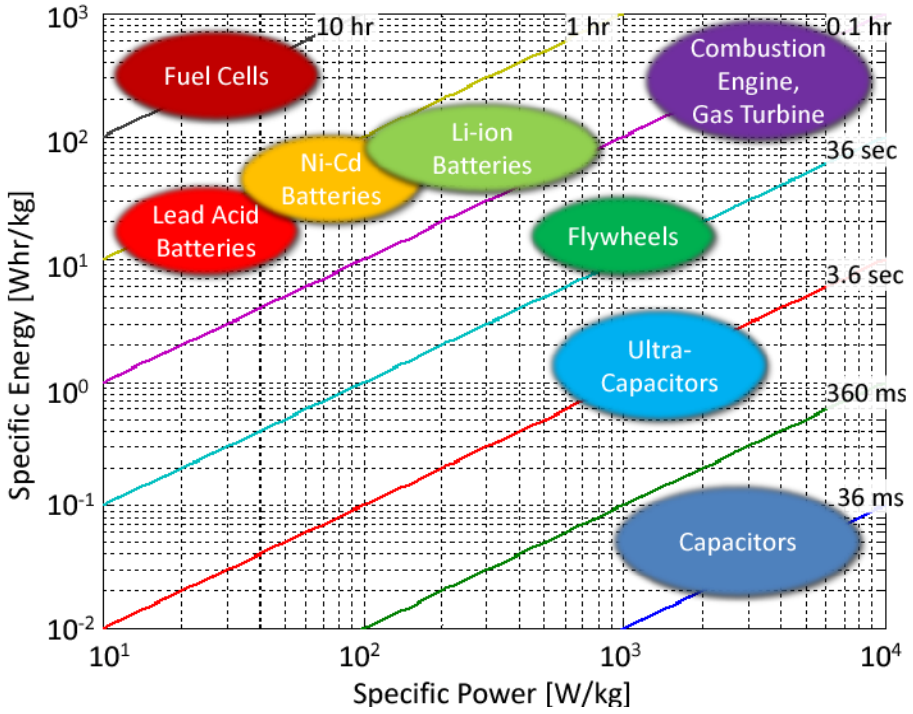

Figure 2.7 Ragone plot [47]

A Ragone plot is a plot used for comparing the energy density of various energy-storing devices [47]. On this plot, the values of specific energy (in W·h/kg) are plotted versus specific power (in W/kg). Both axes are logarithmic, which allows comparing performance of very different devices. The amount of time (in hours) during which a device can be operated at its rated power is given as the ratio between the specific energy (Y-axis) and the specific power (X-axis).

The Ragone plot was first used to compare performance of batteries [47]. However, it is suitable for comparing any energy-storage devices [48] as well as energy devices such as engines, gas turbines, and fuel cells [49].

As shown in the Figure 2.7, each equipment is suitable for a specific application. Fuel Cells are suitable when the load needs small amount of power for a long time (ten hours for

example), because they have low specific power and high specific energy. Batteries are perfect for normal application when a moderate power and energy is needed. They can normally provide power for one hour. Among the batteries, the Li ion batteries can provide more power and energy in respect to their mass. This is one of the most important reasons for their usage in small electronic device but power hungry like smartphones. The Combustion Engine and Gas Turbine are suitable for a load with high power and high energy consumption as they have the highest specific power and specific energy. Flywheels are being used for the fast supply of high power for a short period of time (Almost 36 sec.). Capacitors and ultra-capacitors are being used when a load needs very high power for a very short period of time (Almost for a few milliseconds).

For electrical systems, the following equations are relevant:

$$Specific\ energy = \frac{V.I.t}{m} \quad [W.h/kg] \tag{2.4}$$

$$Specific\ power = \frac{V.I}{m} \quad [W/kg] \tag{2.5}$$

Where V is voltage (V), I is electric current (A), t is time (s) and m is mass (kg).

As the batteries cover wide varieties of applications, they are largely used for different storage solutions, in which the Li-ion batteries are recently becoming the most common battery for energy storage. Hence, a real data of a Li-ion battery providing PCR service is considered for this thesis.

2.4 SOC Models

In the battery management system (BMS), in order to optimize the overall performance of the system, it is necessary to build a lithium-ion battery model with high accuracy and

low computational burden. In addition, it's important to estimate the state of charge (SOC) accurately for battery monitoring and usage, as the battery is a complex, closed system [50]. Therefore, model building and state estimation of Li-ion batteries also play a vital role in BMS [51]. Among all proposed models, there are three main groups which are the most famous ones. They are explained briefly in the following:

2.4.1 Coulomb counting

To date, many approaches have been developed for the estimation of battery SOC, among which Coulomb counting is the most popular technique [52], [53]. In this technique, the current is integrated over time to estimate the battery SOC. Although Coulomb counting is simple and easy to implement, measurement and calculation errors may be accumulated by the integration function, thus reducing accuracy of estimation. In addition, the SOC estimation obtained by this technique is highly dependent on the quality of input initial conditions.

$$\begin{cases} SOC(t) = SOC_{init} & if\ t = 0 \\ SOC(t) = SOC(t-1) + \dfrac{1}{C_n}.\displaystyle\int_{t-1}^{t} i(t).dt & otherwise \end{cases} \tag{2.6}$$

Where $i(t)$ is the DC current in the interval [t − 1, t], positive during the charging cycles of the battery, and C_n is the nominal capacity of the battery, obtained as follows:

$$C_n = \frac{E_n}{V_n} \quad [\text{Ah}] \tag{2.7}$$

2.4.2 Voltage-based method

This approach which is commonly used for the estimation of battery SOC is the voltage-based method [5]. The value of SOC is determined based on a voltage-SOC lookup table,

where the SOC is the function of a measured open circuit voltage (OCV) of the battery. The relation of SOC to open circuit voltage is shown in the Equation (2.8). However, voltage-based methods are not very proper for Li-ion batteries because of their flat plateau of discharge characteristics.

$$SOC(t) = f(E_{ocv}(t)) \tag{2.8}$$

2.4.3 Physics-based methods

These methods are widely used for SOC estimation when the accuracy is the main goal [54], [55]. These methods have intrinsic advantages over traditional Coulomb counting and voltage-based methods. For example, physics-based methods are robust to sensor error and are less dependent on accurate initial SOCs. In physics-based methods, the major problem for real-time SOC estimation is the computational complexity of the coupled partial differential equations (PDEs) which are used to describe the physical processes inside the battery. Simplification of the diffusion PDEs in the solid-phase particles has been found to be the key to reduce the computation time and memory requirement of the physics-based models. The existing methods for diffusion PDE simplification suffer from lots of drawbacks. For instance, the commonly used volume-averaging method can generate unstable equations, which may lead to unacceptable error. Projection-based methods are promising for the model reduction of diffusion PDEs. However, the basis function used in the projection can greatly influence the performance, and how to construct an optimal basis function has not been discussed in the literature. In addition, state filters are required when using a physics-based model for battery SOC estimation. Available state filter algorithms are effective to handle measurement noise and modeling uncertainties. However, these algorithms converge slowly if the initial error is high, which can cause inconvenience to battery users; however, in a recently published papers physics-based electrochemical model is proposed for Li-ion battery SOC estimation involving the battery's internal physical and chemical properties such as lithium concentrations to solve the computationally complex

solid-phase diffusion equations of physical models [56]. An electrochemical model is shown in the following figure

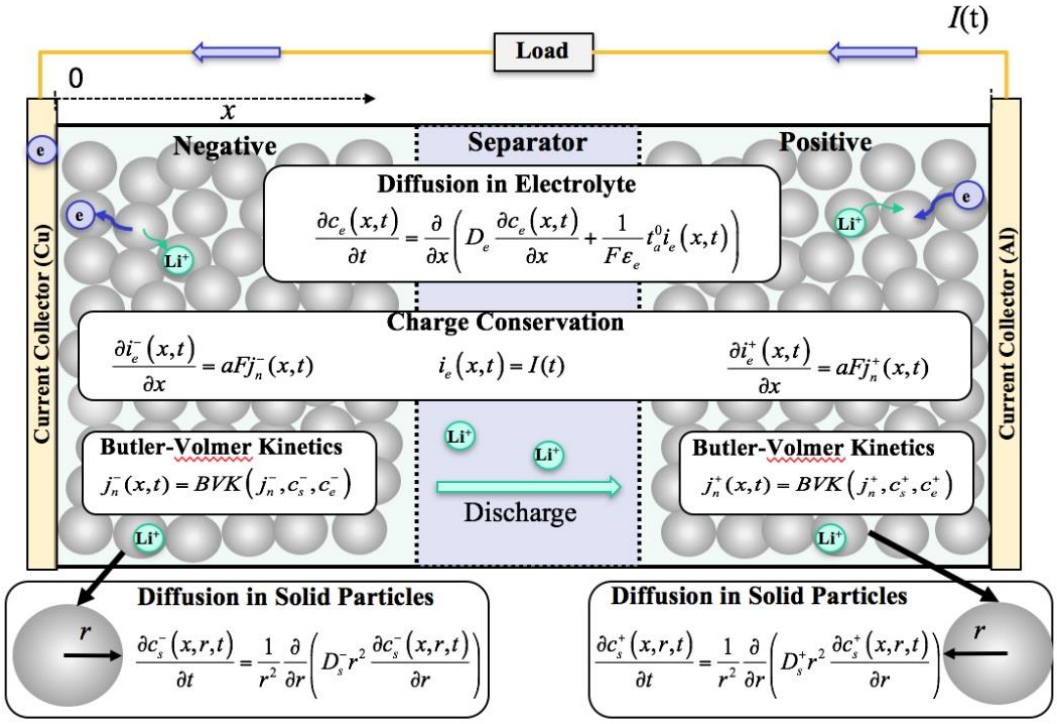

Figure 2.8 Dual-foil battery electrochemical model

2.4.4 Equivalent circuit model (ECM) or Electrical model

The ECM is widely applied to BMS and battery SOC estimation because it is computationally efficient [57], [58]. However, because the ECM is empirical in nature, it provides little insights into the electrochemical process inside the battery, and it cannot provide highly accurate results. It uses electrical circuit components, such as resistors, capacitors, and voltage source to build circuit networks to describe the terminal voltage of batteries. It can describe various dynamic behaviors of the battery accurately. It has good applicability and expansibility, and can be used to develop the model-based SoC estimation approach precisely. Fig.6 presents an ECM with n RC networks, named the NRC model hereafter. The model contains three parts: (i) Voltage source: it uses open circuit voltage

(OCV) to denote battery voltage source. (ii) Ohmic voltage cross the equivalent ohmic resistance R_i, which represents the electrical resistance from various battery components or with the accumulation and dissipation of charge in the electrical double layer. (iii) Dynamic voltage behavior and the mass transport effects: the elements of R_D and C_D are used to describe the diffusion resistance and diffusion capacitance. C_{Di} denotes the i_{th} equivalent diffusion capacitance and R_{Di} denotes the i_{th} equivalent diffusion resistance, U_{Di} is the voltage across C_{Di}, i = 1, 2, 3, 4, . . . n [59]. In figure 2.9, i_L denotes battery load current, U_t denotes battery terminal voltage.

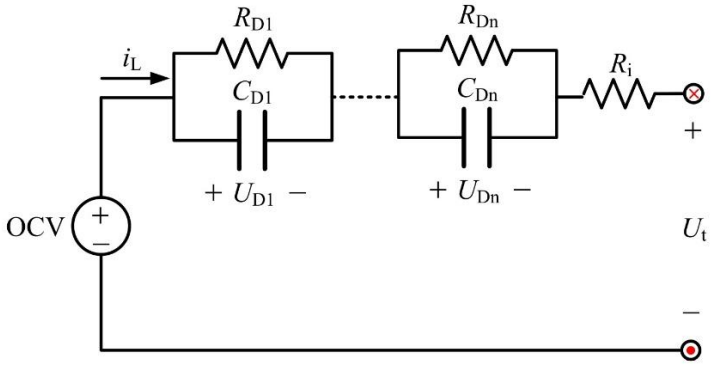

Figure 2.9 Schematic diagram of the NRC ECM [59]

Electrical behavior of the NRC battery model can be expressed by Equation (2.2).

$$\begin{cases} \dot{U}_{Di} = -\dfrac{1}{R_{Di}C_{Di}}U_{Di} + \dfrac{1}{C_{Di}}I_L \\ U_t = U_{oc} - I_L R_i - \sum_{i=1}^{n} U_{Di} \end{cases} \tag{2.9}$$

For working BESS in the safe operating area (SOA), there is a BMS block which controls the voltage, current and temperature of the cells. SOA is a window with safe predefined values for the cell voltages, currents, and temperatures where a battery can operate continuously without any harms or damages [60]. BMS deals with an equivalent

circuit since it works on-line and prevents the battery from detrimental operation by measuring in real-time both voltage and current at terminals.

It is noted that the symbol of battery current is positive during the discharging process and the symbol is negative for charging process. These electrical models can be quite simple as models that take into account only the static behavior or more complex ones that take into account the dynamic behavior as well [61]. Following are the two main subgroup of the model-based SoC estimation with the ECM:

2.4.4.1 Active models

Battery models, in most cases, are composed of a voltage source, whose terminal voltage is a function of the state of charge (SoC), and passive elements, as resistors and capacitors, to model the dynamic behavior of batteries over a certain frequency range [62], [63]. Moreover, these elements can also be functions of other quantities as temperature, current and so on. Figure 10.a shows a simple battery active model.

2.4.4.2 Passive models

supercapacitors are usually modelled using only passive elements as functions of voltage, and possibly, other quantities [64]. In fact, batteries are most of the time modelled as voltage sources because they are seen as dc electric generators, based on chemical phenomena, whilst supercapacitors are seen as large capacitors because their working is based on the charge accumulation phenomenon through the electric field. Even if a battery has chemical reactions, it is electrically equivalent to a big capacitor whose voltage is related to the charge accumulated in chemical way, instead of in electrical way, into the battery itself. For this reason, it is possible to use also for batteries passive models the same as supercapacitors. Figure 10.b shows a simple battery passive model.

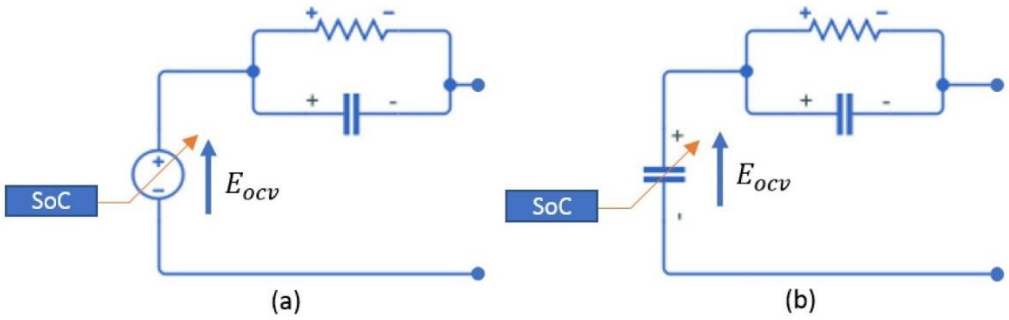

Figure 2.10 (a) Active, and (b) Passive ECM

2.4.4.3 Empirical

It uses the experimental results of a battery pack without the consideration of cell information [65], [66]. The model of this method can be applied to the existing state estimation algorithms for batteries with ease because the model has a simple model structure which is considered in the trade-off between model accuracy and computational complexity. Battery packs usually consist of hundreds of battery cells connected in series and parallel, including battery packs made up of several battery modules, with each battery module containing multiple battery cells in series, parallel, or series-parallel configuration. Going from battery cell model to battery pack model is not simply aggregating cell models to make a pack model, because in this way not only will it introduce unnecessary computational requirements for system simulation, but also because some phenomena that can only be observed in the battery pack are ignored [67]. Significant fidelity loss will occur if inadequate attention is paid to the battery pack behavior, as opposed to cell-level modeling. Thus, it is worth investigating the construction of a battery pack model separately from the cell model.

Three approaches for battery pack modeling are available in the literatures. The first approach is aggregating cell models in series and parallel to represent the battery pack model [68], [69]. This approach requires the least effort going from the cell model to pack model, as the only information needed is the cell configuration in the battery pack. However, serious

loss of fidelity can occur in the resulting battery pack model as a result of ignoring the cell variations, thermal unbalancing in the battery pack, etc. At the same time, in reality not all battery cells used in battery packs are even available to the actual system designers for battery cell modeling.

The second approach is to scale the cell model into a battery pack model with one simplified model representing the battery pack [70], [71]. In this case, the cell discrepancy issues related only to the battery pack are investigated and included in the pack model. Compared with the first approach, the second approach is comprehensive and fast in simulation, which is more suitable for system level design and simulation. Nonetheless, the investigation of cell discrepancy and thermal distribution in a battery pack requires extensive time and effort, and sometimes the battery cells are not readily available to the system designers.

The third approach is building a battery pack model directly on a well-built battery pack with a single battery model capturing the totality of the pack behavior [72], [73]. In this case, the characteristics of the battery cells and thermal influences on them are naturally included into the battery pack model, as a result of cumulative effects of cell averaging, and at the same time the battery model will be fast in simulation requiring comparatively little computational power. Another advantage of this procedure is that non-idealities known to exist in battery packs, such as weak cells and interconnection impedances, is captured self-consistently at the time the battery pack model is built. This approach requires no cell-level details or pack configurations, and some modeling algorithms at this level are even independent of battery chemistry. For commercially available battery packs, this approach may be the only possible approach, as in this case battery tests need only be conducted at the battery pack level. Prerequisites for this approach include 1) the battery cells are reasonably well balanced with means for regular cell balancing, and 2) the battery pack should be effectively cooled/heated so that the battery pack does not encounter uncontrolled temperature variations. In other words, only when a well-designed battery system is available can one confidently model the battery pack as a single battery model. The issue of

battery cells variation has been discussed in many papers and communications [70]- [74], and a two-step screening process has been proposed in [70] to ensure a stable configuration of a battery pack, and many cell equalizations approaches have been proposed as well [75], [76]. Comparing the three battery pack modeling approaches discussed above, the third approach which builds a battery pack model directly on battery pack terminal measurements seems to be the most promising for system level designer. However, large modeling errors up to 3.1% for this battery pack modeling approach even with moderate real-world test regimes were reported in the literatures [72], [73], which needs to be improved for stringent high-fidelity system level simulations.

Chapter 3

Ancillary Services Market (ASM)

Ancillary Services (AS) is an essential element in any electricity market design. The Independent System Operator (ISO) relies on AS to ensure system security and reliability. AS usually include regulation up (Reg-Up), regulation down (Reg-Down), spinning reserve (Spin), nonspinning reserve (Non-Spin), voltage support, and black start. In some markets, AS products are broken in different categories such as 6 second raise, 6 second lower, 60 second raise and 60 second lower, 30 minutes standby, etc. Operating reserves, i.e., regulation, spin and non-spin, are usually procured through competitive markets. Bidders submit AS bids and then the market clearing price is found as the price where supply is equal to demand. All offers at or below the clearing price are accepted. Voltage support and black start services are usually procured by resource specific agreements between the Independent System Operator (ISO) and the suppliers. A generator must meet certain performance criteria in order to be eligible for providing a specific AS. For example, a generator must be equipped with Automatic Generator Control (AGC) devices in order to provide regulation services. Furthermore, the amount of capacity that a unit can provide is limited by the unit's operating characteristics, such as ramping capability. The minimum performance requirements for

each ancillary service are usually specified by national reliability organizations such as NERC (North America Reliability Council) [77].

3.1 Electricity Market Regulations

The Day-Ahead Market (DAM) is an electricity market that works one day in advance with respect to the actual delivery time. It lets “financial” and “physical” trading. A financial market lets participants to buy or sell energy on the market, with no actual delivery obligation. A financial transfer is related to any energies that is not delivered. On the other side, a physical market related to any trading which is corresponded to an actual transfer of power. The DAM provides both financial and physical participation [78]. The DAM is an auction market and it is not a continuous trading market. It hosts most of the transactions of purchase and sale of electricity. Producers as sellers and consumers as buyers place their offer in an Electricity Pool, which is managed by a central entity called Power Exchange (in Italy, Gestore dei Mercati Energetici - GME). The Power Exchange (PX) represents the only counterparty for the market players, by acting as the only buyer for producers and the only seller for consumers [79]. Note that when buyers and sellers communicate with the PX, they do not know whom they are dealing with.

3.1.1 Basic D-ahead market trading principle [80]

- Calculations are made simultaneously for 24 hours of supply for all bids and quotations.
- Prices are set for each hour separately. Equilibrium price is set with the help of special software.
- **Pricing principles are as follows:**
    - Supply and demand curves are formed for each hour of the day in €/MWh.
    - The intersection of the curves determines the equilibrium price.

- Market operator is a central contractor for all sale and purchase deals. Each participant either sells or buys the needed volumes of electricity from the market operator.
- In the Day-ahead market, participants make bids and offers for the purchase and sale of electricity respectively during one or more accounting periods (hours of the day).
- Billing and settlements under agreements are made by the market operator.

Figure 3.1 shows the procedure of finding of clearing price (cut-off price) for Day-ahead market:

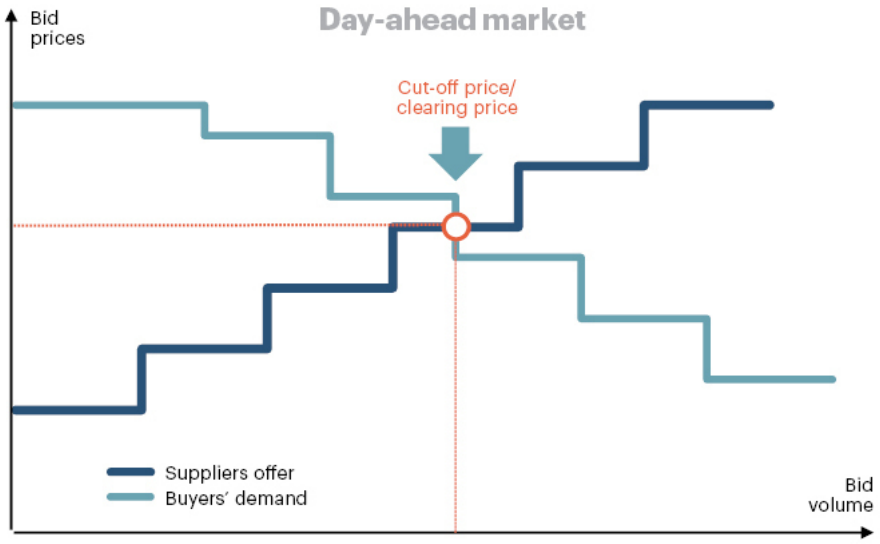

Figure 3.1 Equilibrium point for Day-ahead market [80]

3.2 Ancillary services

Ancillary services are support, generally referred services other than energy that to those are essential for ensuring the reliable operation of electric power losses, black start capacity, systems [81]. According to this definition, many services such as frequency regulation, voltage regulation, system restoration, load shedding and reserves with varying levels of

response time are considered as ancillary services. However, many entities such as Federal Energy Regulatory commission (FERC), North America Electric Reliability council (NERC) and Oak Ridge National Laboratory (ORNL) have developed comprehensive lists of ancillary services [82], [83]. These organizations are related to the USA power system where the nominal frequency for the power systems is 60 Hz. In Europe, the reliability organizations are the national regulatory authorities (NRAs). Transmission System Operator (TSO) is an organization responsible for transporting energy in the form of natural gas or electrical power on a national or regional level, using fixed infrastructure in the Europe. The term is defined by the European Commission. The standard for the nominal frequency for the power systems in Europe is 50 Hz (In the simulation of this work, 50 Hz is the nominal value). TSO in Europe is the same as ISO in the USA.

The power system has metamorphosis in recent years, as a result of the steady growth of renewable energy sources like solar, geothermal, and wind power in the generation mix. Although this brings great advantage as result of its natural eco friendliness, however, unlike, generators, the uncontrollability of RE poses a major challenge to system operators. BESS, on the other hand, is greatly welcomed by system operators because of its advantage of its large energy storage functionality [84]. The enormousness of BESS applications includes, but not limited to: intermittency compensation of renewable energy, frequency regulation, transient stability, voltage support, frequency compensation, frequency regulation, load leveling, spinning reserve, uninterruptable power supply (UPS), and improvement of energy. Although it is most actively developed due to its colossal applications, expensive initial investment cost and limited lifetime are still to its commercialization. However, many such projects are still ongoing for frequency regulation, because of its economic viability [85]. Fast response due to BESS is suitable for frequency regulation and has proven to be superior to existing generators in recent research [86]. In the following, some of the most important ancillary services are explained:

3.2.1 Frequency regulation

The system frequency is the heartbeat of the grid. It indicates the balance between power supply and demand of the system. System frequency fluctuations are caused by supply-demand imbalance on the grid. Frequency fluctuations occurs at the instance of sudden power fluctuation. System frequency and demand power shows high correlation at every instance in time. As shown in Figure 3.2, at any given time period, system frequency depicts an inverse proportion with demand power. This is as a result the frequency falls when the demand power rises and the frequency rises when the demand power falls. So, If the balance between generation and demand is not reached, the system frequency will change at a rate initially determined by the inertia of the total system. The total system inertia comprises the combined inertia of most of the spinning generation and load connected to the power system [87]. It should be note that even though the nominal frequency of the Figure 3.2 is 60 Hz, the nominal frequency chosen for the simulation in this work is 50 Hz.

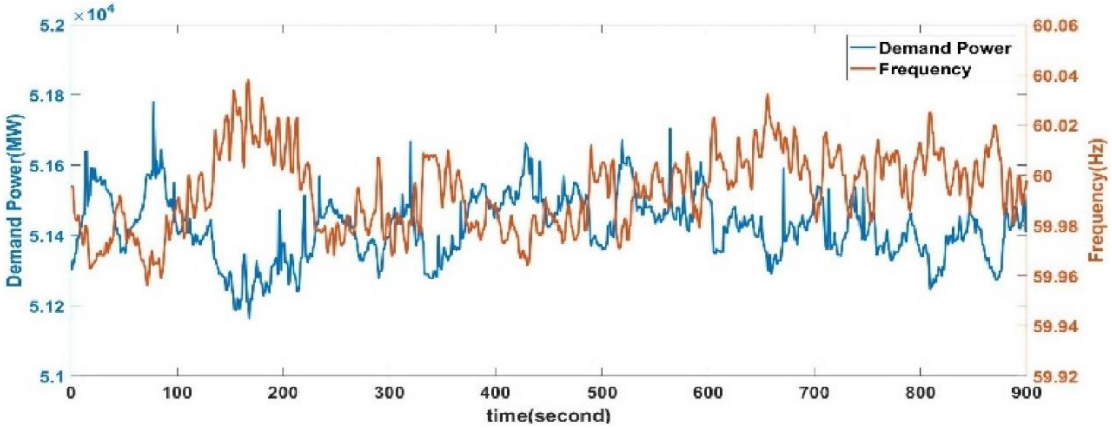

Figure 3.2 Frequency variation vs. demand power [88]

Low levels of rotational inertia in a power system, caused in particular by high shares of inverter-connected renewable energy sources (RES), i.e. wind turbines, and PV panels which normally do not provide any rotational inertia, have implications on the grid's frequency dynamics. This can lead to situations in which traditional frequency control schemes become too slow with respect to the disturbance dynamics for preventing large frequency deviations and the resulting consequences.

The loss of rotational inertia, and its increasing time-variance, leads to new frequency instability phenomena in power systems. Frequency and power system stability may be at risk. If, during a system frequency disturbance, the balance between generation and demand is not maintained, the system's frequency will change at a rate initially determined by the total system's inertia. The total system's inertia comprises the combined inertia of most of the spinning generation and load connected to the power system. The contribution of system inertia of a load or generator is dependent on whether the system frequency causes changes in its rotational speed and, therefore, its kinetic energy. The power associated with this change in kinetic energy is fed by, or taken from, the power system and is known as the "inertial response" [89]. Figure 3.3 shows the typical inertial response requirements of a grid.

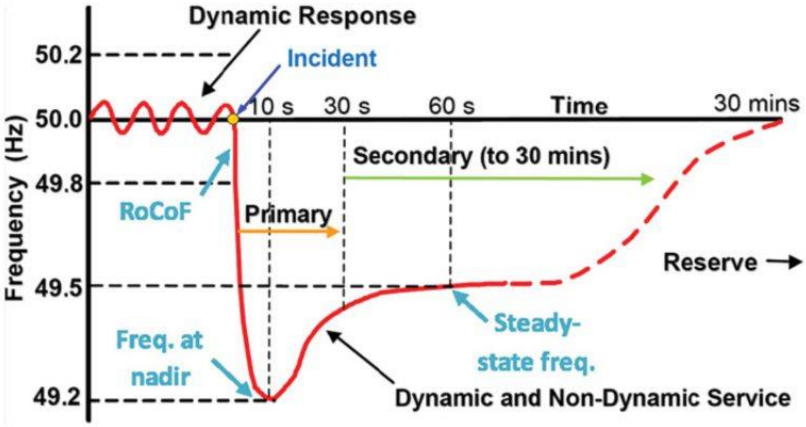

Figure 3.3 Grid inertial response [90]

During a system frequency event the total inertial response of all electrical machines connected to the system determines the initial rate of change of frequency (ROCOF).

For a robust power system (system frequency is not overly sensitive to power imbalances), it is extremely important that a large proportion of generation and load connected to the power system contributes to the system's total inertia and then provides inertia response.

Inertial power rating and energy will depend on what is required by the network, and is dependent on the level of power to be supplied to the network in the instant between failure and adjustment of remaining plant to take up the load. The control of a large power system is hierarchical. In this discussion, three frequency control services (primary control, secondary control, and tertiary control) are explained, but our focus is on primary control action.

3.2.1.1 Primary Control Reserve (PCR)

Transient imbalances between generation and consumption induce deviations of the frequency. The main purpose of primary frequency control (PFC) is to react within a few seconds to any frequency deviation higher than ±20mHz to keep frequency variation within the maximum threshold (±200mHz) and re-establish the balance between produced and consumed energy. Currently detection of these deviations is used to tune generators (that participate to this primary frequency control) according to their available power reserve. The same control function can be implemented into the control system of the grid connected power converter, which is embedded in the BESS. From an economic point of view the interest is that the revenue from this given service is constant and warrantied [91].

Load frequency control (LFC) is a term applied to describe the continuous operation of keeping the frequency of a power system stable. The frequency of a power system is connected to the balancing of produced and consumed power in the way that if there is a surplus of produced power the frequency will rise, and if there is a lack of produced power the frequency will fall. It is very important that this power balance is maintained, if not the generators could lose synchronism, and the power system would collapse. As shown in Figure 3.4, LFC has a hierarchical structure with primary and secondary, and tertiary control.

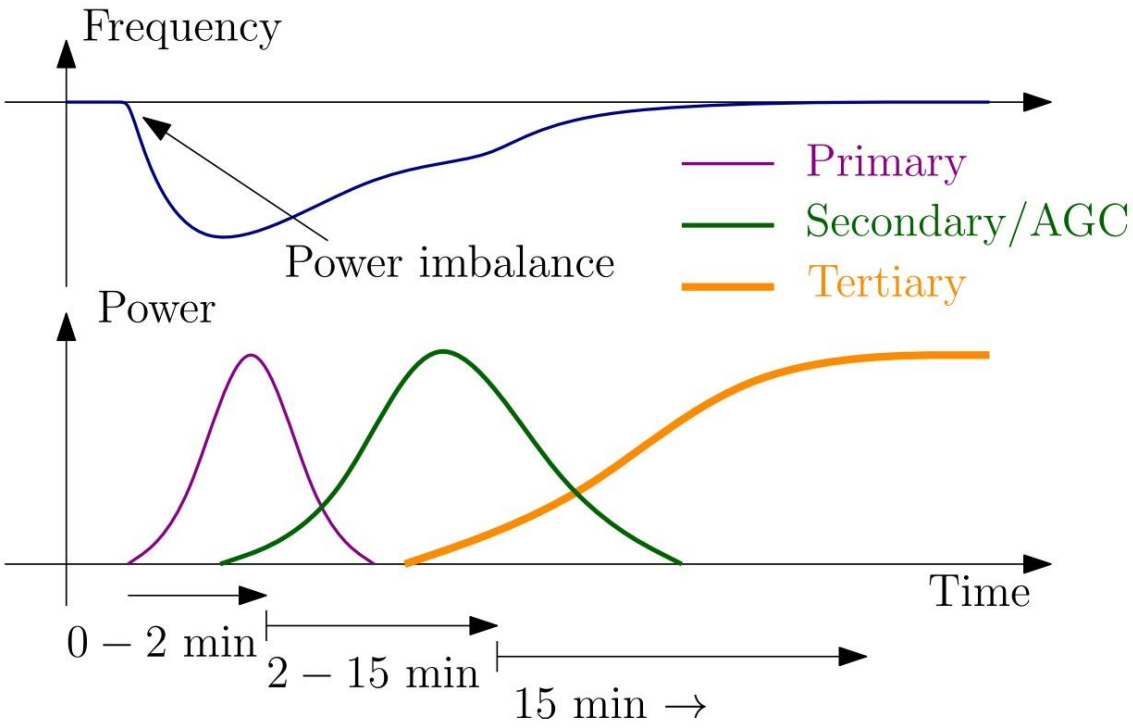

Figure 3.4 Activation of primary, secondary, and tertiary control after a power imbalance [92].

PCR acts as follow:

1. In case of under frequency, positive reserve injects power in the grid.
2. In case of over frequency, negative reserve absorb power from grid. Actually, all relevant units inject less power than programmed in grid.

The final goal for PCR is to achieve:

$$\sum E_{produced} = \sum E_{consumed} \tag{3.1}$$

Which means the frequency of the grid gets its optimal initial value (50Hz or 60Hz). PCR is a mandatory service which has to be provided by every production units with apparent power greater than 10MVA. These units are called Relevant Production Units

(RPU). PCR is not subject to ASM, but it is remunerated according to the price of electricity in that zone.

3.2.1.1.1 The BESS Controller

In this study, designing of a new controller is not the case. Within this framework, the controller is only used for:

• directly receiving the power setpoints (P_{gridAC}) from input time-series. This occurs during the verification, where the BESS model must operate on a cycle of the user's choice;

• converting frequency deviation into a power setpoint via a droop control curve. This occurs during the validation process, where the BESS model is tested via frequency regulation cycles. The droop control curve is built in the model controller based on the curve controlling the operation of a real battery under study while providing frequency regulation. It is a simplified control curve, defined in Equation (3.2) and presented in Figure 4.5, featuring no dead band and a droop value of 0.69%. The utilization of a droop curve without a dead band could be a decrement in the test duration due to the its incrementation in energy flow during the test. This is suitable for the validation process since its purpose is to investigate the estimation error rather than the effectiveness of the control strategy. computed as follows:

$$droop = -\frac{\frac{dF}{F_n}}{\frac{dP}{P_n}} \times 100 \quad [\%] \tag{3.2}$$

where *dF* is the frequency deviation (in Hz), *Fn* is the network nominal frequency of 50 Hz, *dP* is the power setpoint (in kW), and *Pn* is the nominal power of BESS (in kW).

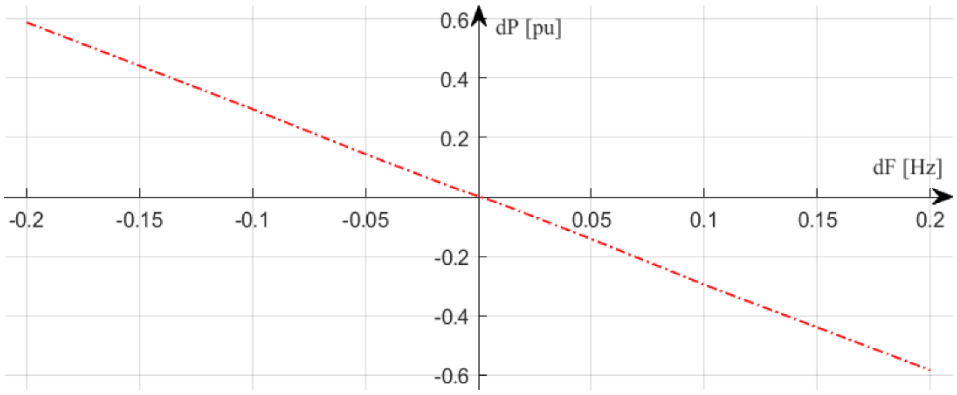

Figure 3.5 Droop control curve for frequency regulation

3.2.1.2 Secondary Control Reserve (SCR)

Secondary frequency control, also referred to as load frequency control (LFC), is the second level for compensating an active power mismatch. After PCR reached to its maximum power delivery, SCR starts and must achieve to its nominal value within 15 minutes. If it does not, tertiary control takes over from secondary control. As opposed to primary control, secondary control reacts only to a disturbance in the LFC's own control area in order not to change the load flows on tie-lines to other areas. It can be either performed manually or automatically. PCR can only interrupts deviation and reach to a steady-state frequency value which is higher or lower, depending on the situation, than the nominal value. It cannot restore frequency to the optimal nominal value. SCR causes an unbalance in grid for a certain period of time. It is injecting power if frequency is below the nominal value and absorbing power in case frequency is above nominal value.

SCR is not mandatory, and each provider is required to have high power set points as the number of providers are not many. They must offer the same power band for positive and negative reserve: SCR is a symmetric service. In order to avoid any constraints, TSO given the total available quantity of PCR and calculates the total power required to restore the nominal value of frequency and shares it among all the providers. In Italy, the TSO

defines each minute a signal, called Area Control Error (ACE - Livello Regolazione Secondaria is the Italian name), which is valid simultaneously for all providers. It represents the percentage of power reserve required to each production unit selected in the market [93]. The scale for the ACE signal is a number between 0 and 100 [94].

$$\begin{cases} \Delta P = \Delta P_{SCR} & if\ ACE = 100 \\ \Delta P = 0 & if\ ACE = 50 \\ \Delta P = -\Delta P_{SCR} & if\ ACE = 0 \end{cases} \tag{3.3}$$

3.2.1.3 Tertiary Control Reserve (TCR)

It also known as manual frequency restoration reserve (mFRR), frequency restoration reserves (FRR), and replacement reserves (RR). In case of necessity, tertiary control reserves are manually activated within 15 min by the TSO. It is primarily activated to free secondary reserves in a balanced situation, but also to support secondary control after a large incident to restore the frequency to the nominal value and prevent the need of primary control. Tertiary control reserves have to run until the generation is re-scheduled to fit the new system situation [92].

In Italy, this service is centrally coordinated by Terna and traded on Ancillary Services Market. It requires slower but longer action (as shown in Figure 3.4); hence, it has a slow ramp and a large energy output.

3.2.2 Voltage Control

Distribution networks have not been designed to cope with power injections from Distributed grid (DG), therefore the proliferation of DG on the electric networks results in a number of adverse impacts, including voltage variation, degraded protection, altered transient stability, bi-directional power flow and increased fault level, the voltage variation

has been addressed as the dominant effect [95]. Typically, one of the most severe situations is that voltage magnitude at the proximity of DG exceeds the statutory limits during maximum power output from DG and minimum power demand from the network. Here the network experiences the largest reverse power flow and large voltage change which affects the network safety and stability.

Distribution network operators (DNOs) are responsible for operating the network within statutory limits. The voltage variation problem can be solved by either network, generator or load operational changes (utilizing the existing infrastructure) or network asset upgrades [95]. The network and generator operational changes, such as DG power curtailment, may conflict with contractual policies ("first on last off") between DNOs and DG. Whilst the network asset upgrades, such as reinforcement of networks, require significant investments on the distribution networks. DNOs need to justify the cost in terms of revenue benefit [96].

3.2.3 System Restoration

The objectives of restoration are to enable the power system to return to normal conditions securely and rapidly, minimize losses and restoration time, and diminish adverse impacts on society. Many non-structured methods and technologies and object-oriented expert system have been employed in making restoration schemes to address the above objectives, but the establishment and maintenance of a knowledge base of past restorations remains a bottleneck [97].

Wind and solar power as clean and renewable energy are significantly adopted but they are inherently volatile, intermittent and random. Therefore, an improper handling of certain partial failures can easily lead to accidents and severe chain reactions, and thus may cause large-scale/extensive blackout eventually. Large-scale blackout risks still exist and are inevitable, although a great amount of work has been done to make power systems resilient against outages [98]. A proper restoration plan can effectively mitigate the negative impact

on the public, the economy, and the power system itself. Research on how to restore the power system quickly and effectively after outages is of vital significance.

Power system restoration after a partial or complete collapse is quite a complex process. Many factors need to be considered including the operating status of the system, the equipment availability, the restoration time and the success rate of operation. It needs not only a large amount of analysis and verification, but also decisions made by dispatching personnel. Power system restoration is a multi-objective, multi-stage, multi-variable and multi-constraint optimization issue, and is full of non-linearity and uncertainty. It can be described as a typical semi-structured decision-making and it is difficult to obtain a complete solution [99].

3.3 BESS for Ancillary Services Provision

In the Nordic Network, the TSOs aim at keeping the frequency between 49.9 and 50.1 Hz. This has proven to be increasingly difficult, and as seen from Figure 3.6, the number of frequency incidents (minutes spent outside 49.9 and 50.1 Hz) has increased concurrently with installed wind power capacity over the last decade. It is confirmed by Statnett, the Norwegian TSO, that the increasing amount of intermittent energy resources is part of the reason for the decreasing control performance, along with a heavier loaded network and an increasing amount of bottlenecks, which at times excludes some of the resources from participating in LFC [100]. There have been many suggestions to how LFC can be improved to better cope with these challenges. In some literatures, loads are included in LFC [101], [102], while [103] concentrated on effective energy storage. BESS can absorb energy during periods of high frequency and dispatch energy during periods of low frequency. A fairly complex control algorithm is required to ensure that the BESS is capable of performing either function when required [90].

Energy support for frequency management is short in nature and many solutions are based on super- and ultra-capacitors. Ultra-capacitors are well-suited to supply as such a

pulse of power. The reason is obvious: high energy discharge capability and long life. Synthetic inertia generation using ultra-capacitors has been demonstrated successfully on grids such as in island networks [104], and the extension to micro-grids and larger smart grids using DESS is a distinct possibility which has been considered by numerous networks, but super capacitors are more expensive and unmatured technology compared to BESS. Therefore, most of the stationary energy storages are based on BESS especially Li-ion batteries.

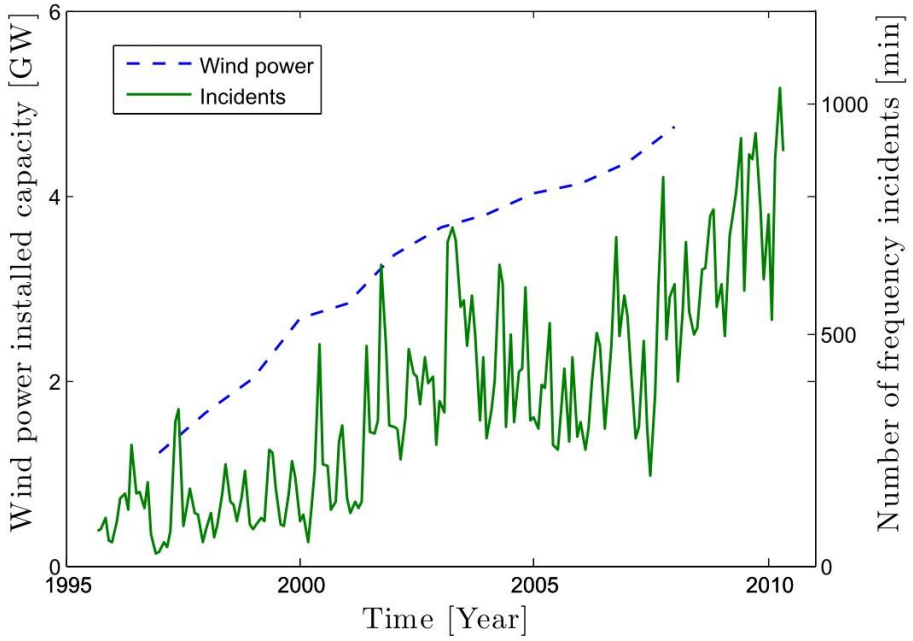

Figure 3.6 Number of frequency incidents per month [105] and installed wind power capacity in the Nordic system [106].

While battery energy storage technologies can cover a wide spectrum of applications, ranging from short-time power quality support to hours-long energy management, the supply of primary control reserve has been identified as the application with the highest value for the owner of the BESS. The focus is on short-duration storage technologies which can be used to assist in primary frequency control. Storage technologies that suit such applications, typically grid-scale batteries, can respond at a much faster rate than the mechanical actions of traditional governor controls and blade pitch or wind turbine speed control mechanisms. However, economic concerns suggest that such storage will be very limited in the amount

of power it can provide [107]. According to all aforementioned reasons, a Li-ion BESS is investigated for this study.

Chapter 4

Methodology

Many stakeholders, governments, and researchers are interested in simulating the real behavior of BESS. As already explained, several models of electrochemical, electrical, and empirical models are already developed for SOC estimation, but most of them are based on ideal characteristic of the batteries. Hence, they are not based on the real behavior of a battery, and in reality, they show a big error in SOC estimation. One the common models for SOC estimation is electrical model. It deals with voltage and current as the inputs of the Battery management system (BMS). It is less accurate than electrochemical model, but faster in simulation elapsed time. If the monitoring and controlling of electrical parameters is not required, empirical models can be a good option. They employ past experimental data for estimating the future behavior of BESS. Polynomial functions are usually used as empirical models [108]. Empirical models have already successfully used for SOC estimation. They not only have estimated the behavior of the battery with an acceptable accuracy, but also decreased the computational effort tremendously in compared to the electrical model [6]. In this study, a novel empirical model based on lumped elements characterized by parameters estimated via an experimental campaign is developed instead of using polynomial functions.

The main outcome of such strategy would be a more realistic SOC estimation model. The main elements of this model are explained in the following.

4.1 Empirical Model for PCR provision

The developed model is shown in the Figure 4.1. It is made of two main blocks which are PCR controller and BESS Empirical model. They are designed in Simulink.

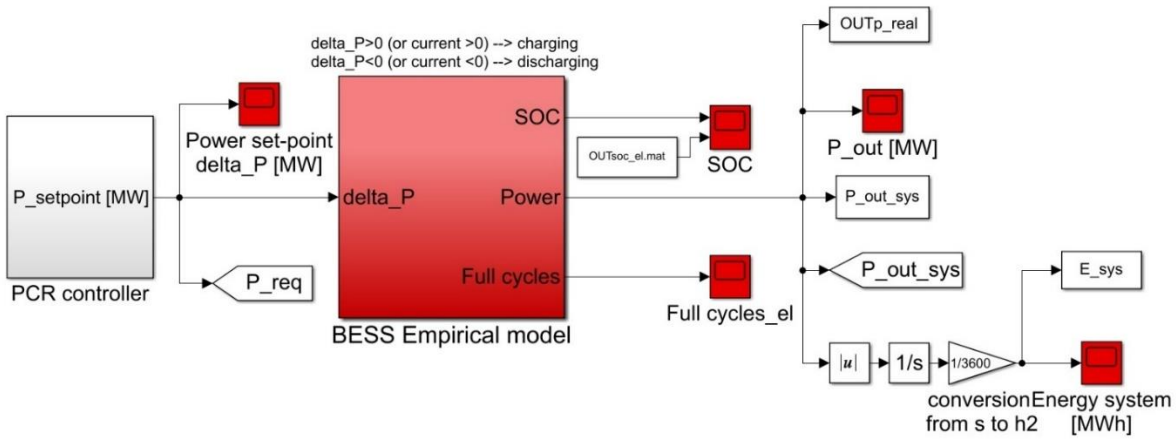

Figure 4.1 Empirical Model for PCR Provision

4.2 PCR controller

A Controller makes the BESS operation strategy in runtime. It receives frequency profile of the grid as the inputs. It calculates the power setpoint requested from the grid to the BESS (P_{gridAC}) as the output and deliver it to the BESS block. The sampling rate of the output can be configured by user. The reason for using this block is to prepare the power profile so that the system can provide an ancillary service which is PCR for this study; for example, scaling the sampling rate of data from second to hour for analyzing services in hour timescale.

4.3 BESS Empirical model

The battery pack is the main core of the BESS model. The BESS overall efficiency (η_{BESS}) varies with P_{gridAC} and SOC. The efficiency of the operation highly depends on the requested power and on the amount of energy available in the battery at each moment, because of the electrochemical structure of batteries. Our model calculates an overall efficiency instead of two separately calculated efficiencies for power conversion and for battery cycling. This choice has two main reasons. First, without compromising the accuracy of the model, its complexity decreases. Second, utilization of higher accuracy of AC measurements. Inside the BESS empirical model block is shown in the Figure 4.2.

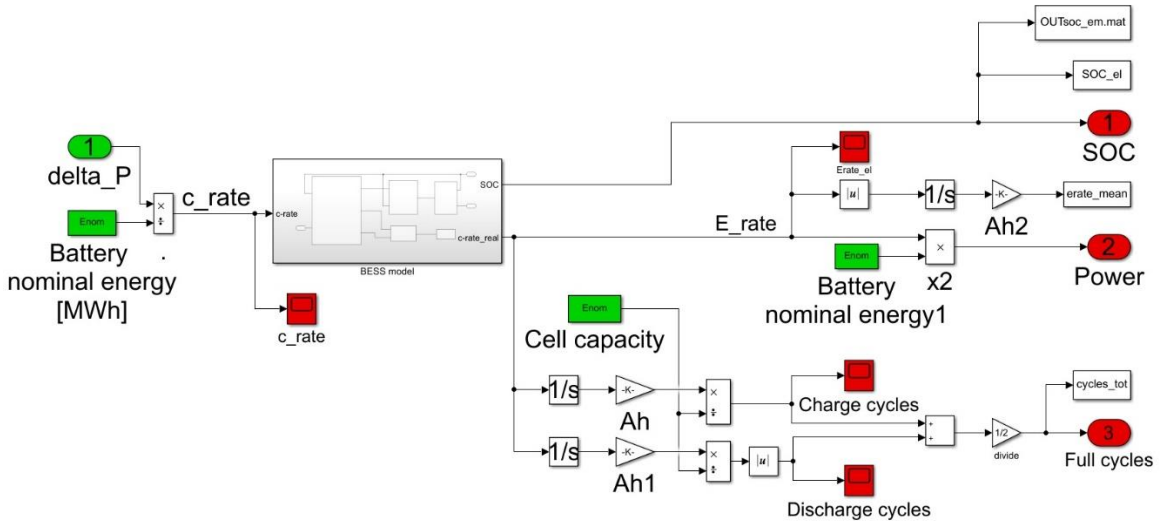

Figure 4.2 BESS model

4.3.1 BESS model

The BESS model consists of Overall efficiency, Capability curve, SOC update, and Efficiency computation blocks. Its subblocks are shown in the Figure 4.3. In the following, all Different blocks are explained in detail.

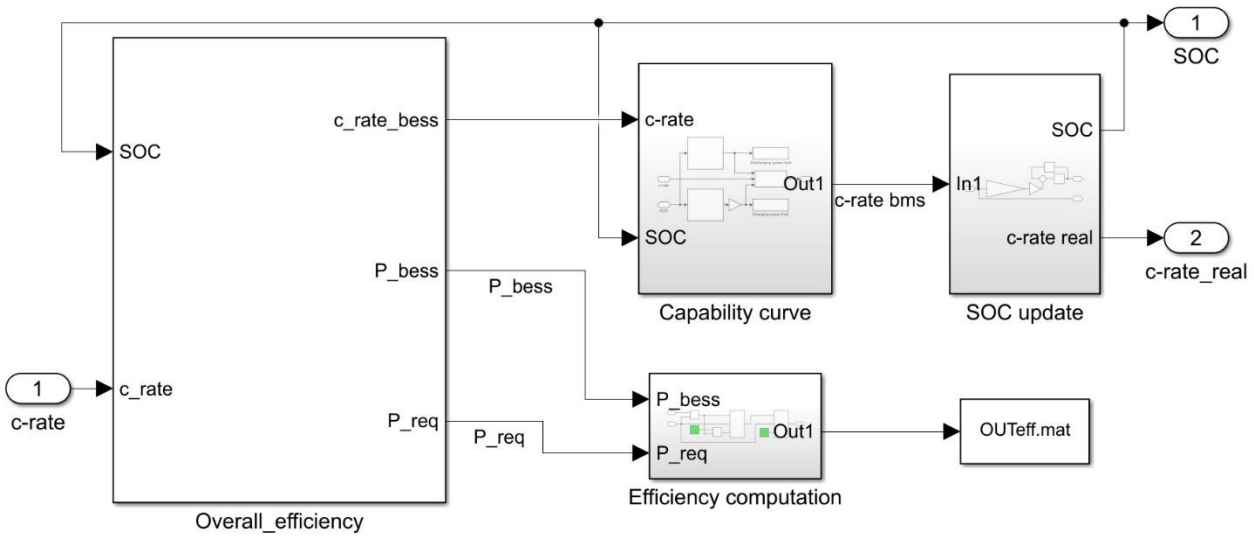

Figure 4.3 BESS Model Subblocks

4.3.1.1 Overall efficiency

As shown in the Figure 4.4, this block has a main block named BESS efficiency. The overall storage and conversion process efficiency is the main outcome of the experimental campaign. The η_{BESS} is computed as a function of P_{gridAC} and SOC. It is obtained as an outcome of a test [109]. The η_{BESS} is the ratio between energy injected and energy absorbed through cycles. The related curve of the η_{BESS} is illustrated in Figure 4.5, obtained from a linear interpolation of the experimental outcomes on the domain.

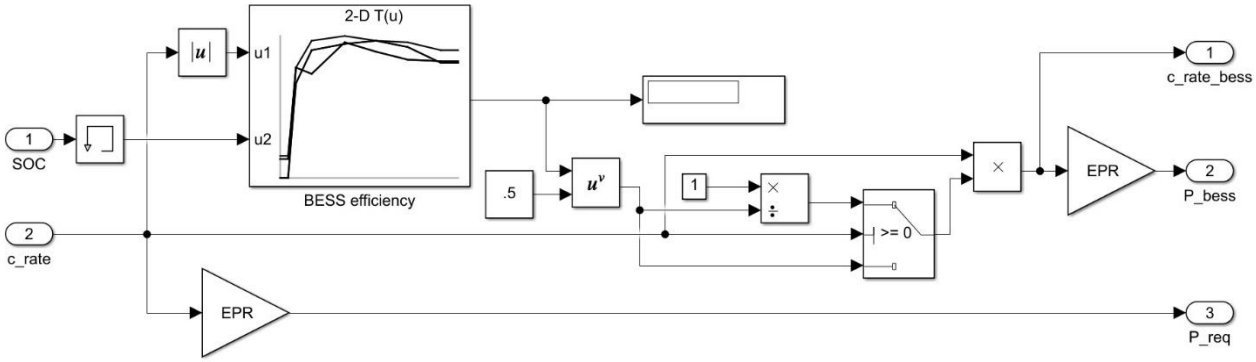

Figure 4.4 Overall efficiency

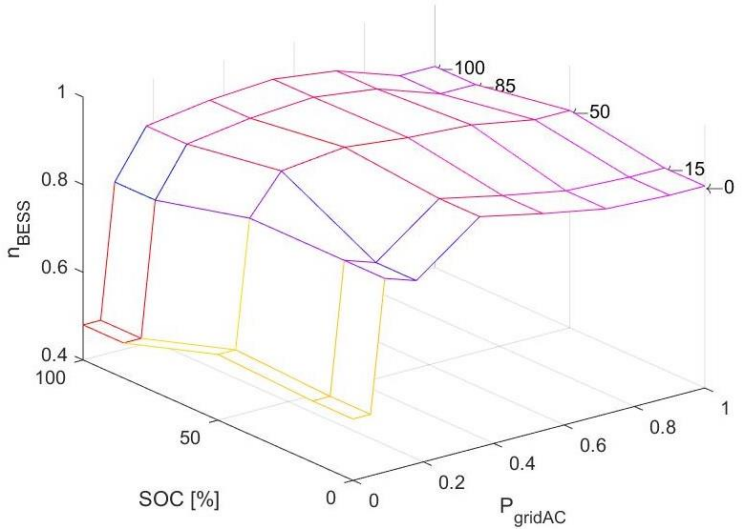

Figure 4.5 The curve of the η_{BESS}

The system efficiency is generally high (around 90%). The η_{BESS} heavily depends on the amount of the requested power from the battery, for example, at low power, power conversion system (PCS) losses increase dramatically and the efficiency sharply decreases. At high power, phenomena inside the electrochemical cells are responsible to diminish a bit the efficiency. The best situation which causes the highest η_{BESS} is SOC close to 50%. Efficiency is implemented in the model as a Lookup table (LUT). The LUT is presented in Table 4.1.

Table 4.1 BESS efficiency lookup table as implemented in the model

η_{BESS}	SOC [%]				
P_{gridAC} [per unit]	**0**	**15**	**50**	**85**	**100**
0.00	0.540	0.540	0.550	0.480	0.480
0.05	0.540	0.540	0.550	0.480	0.480
0.09	0.842	0.842	0.842	0.787	0.787
0.18	0.818	0.818	0.931	0.896	0.896
0.36	0.926	0.926	0.947	0.917	0.917
0.54	0.895	0.895	0.931	0.927	0.927
0.72	0.868	0.868	0.922	0.908	0.908
0.90	0.861	0.861	0.896	0.859	0.859
1.00	0.861	0.861	0.896	0.859	0.859

4.3.1.2 Capability curve

The BESS model features a capability curve block for the active power of the battery. It is shown in Figure 4.6. In order to safely absorb or inject different levels of power by battery, capability curve block is limiting the charging power when the SOC is getting higher than 96% or discharging power when the SOC of the battery is getting lower than 4%. This process is implemented by two one-dimensional lookup tables, one for Charging cycles and the other one for discharging cycles, plus a saturation dynamic block. This saturation block bounds the range of the battery power into an acceptable value by using the upper and lower limits. The Capability lookup tables are implemented in graphical forms which are presented in Figure 4.7.

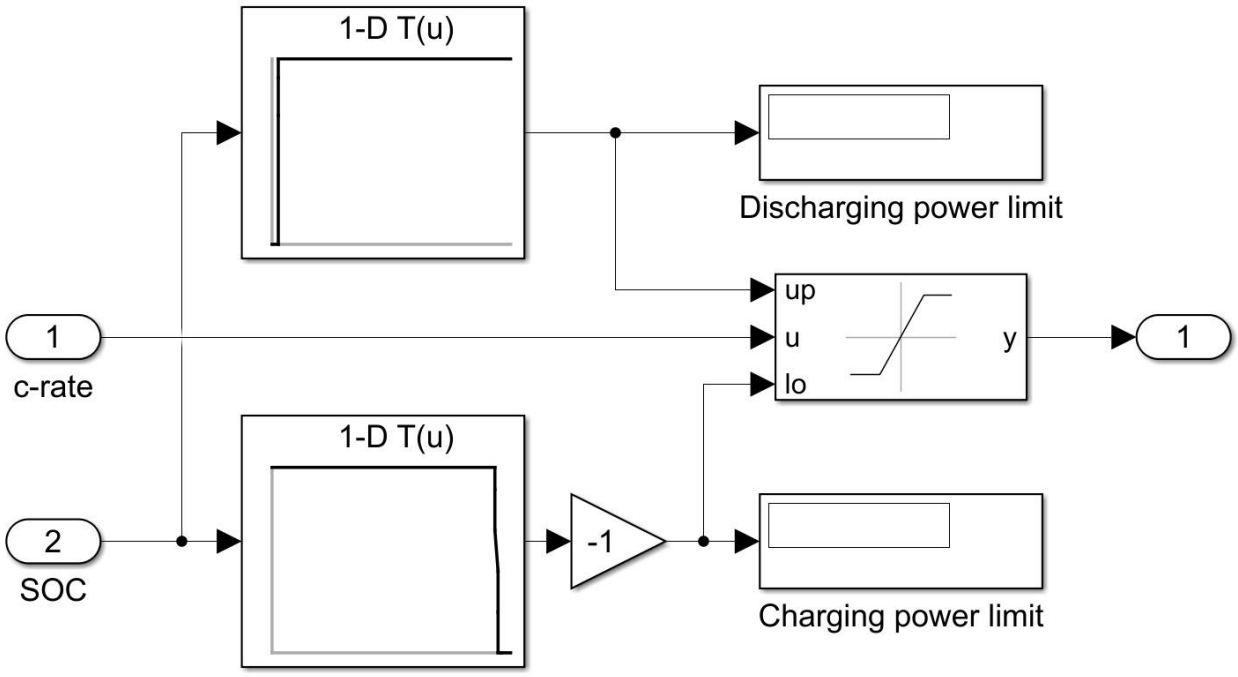

Figure 4.6 Capability curve block

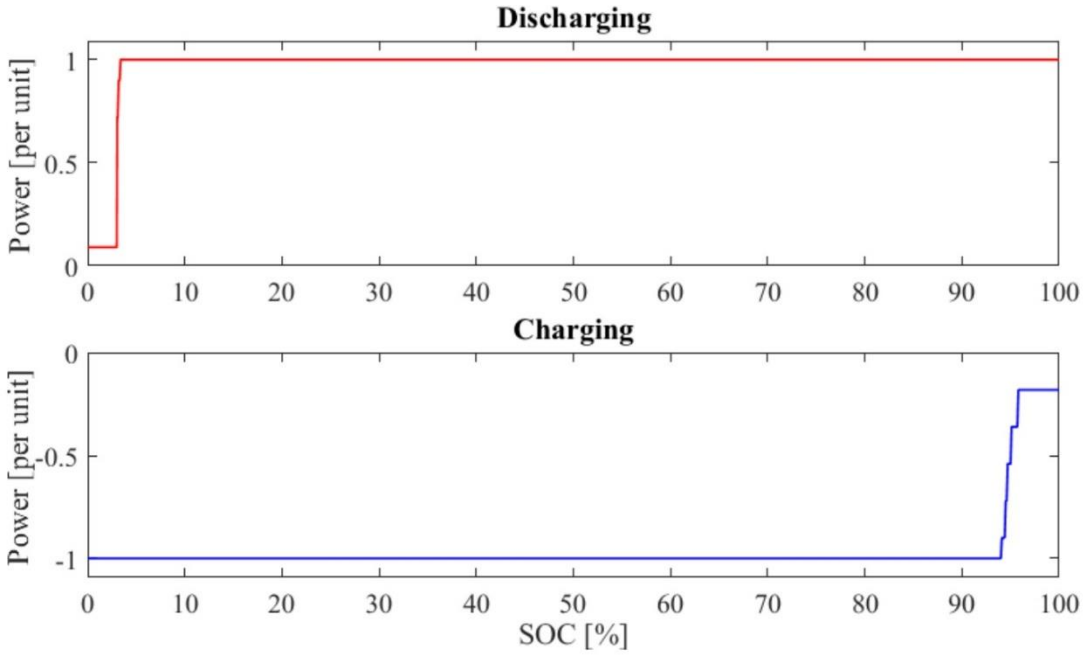

Figure 4.7 Capability lookup tables

4.3.1.3 SOC update

This block receives c-rate as an input and deliver the SOC as an output. It made up of gain, memory and saturation blocks. The value of the input c-rate is changed into hour in percent with the gain blocks. Then, this value subtracts from the value comes from memory block through a feedback to give the SOC. The memory block keeps the value of the SOC of the last sample [time: t-1], and sum it with current value of the SOC variation [time: t] to calculate the current SOC. At the end, this SOC bounds to a new value between SOC maximum and SOC minimum. All these blocks are illustrated in Figure 4.8.

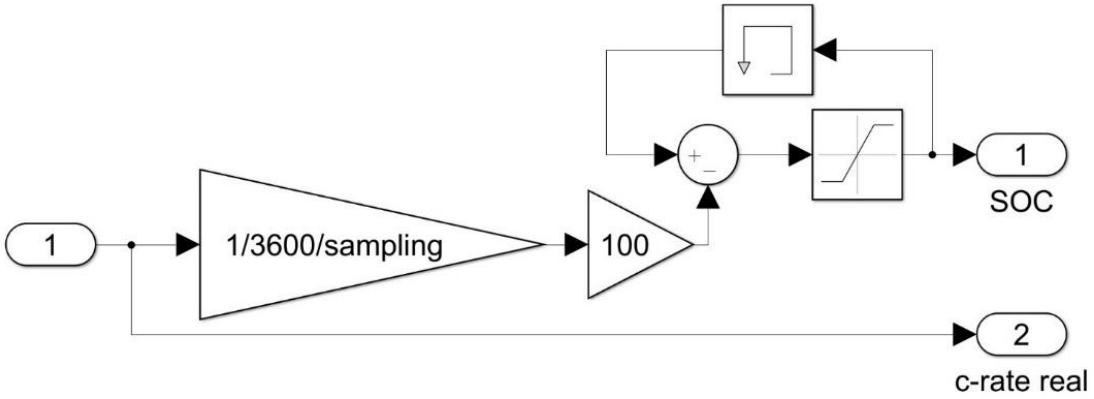

Figure 4.8 SOC update

4.3.1.4 Efficiency computation

The efficiency of the BESS is the ratio of the output power of the BESS (P_{BESS}), and the requested power from the grid P_{req}. It is formulated as follow for each single moment:

$$\eta_{BESS} = \begin{cases} \frac{P_{req}}{P_{BESS}} & P_{req} > 0; \\ 0 & P_{req} = 0; \\ \frac{P_{BESS}}{P_{req}} & P_{req} < 0; \end{cases} \tag{4.1}$$

According to the upper formula, the η_{BESS} is implemented in Figure 4.9. The final value for the η_{BESS} is the mean value of all data collected in this block.

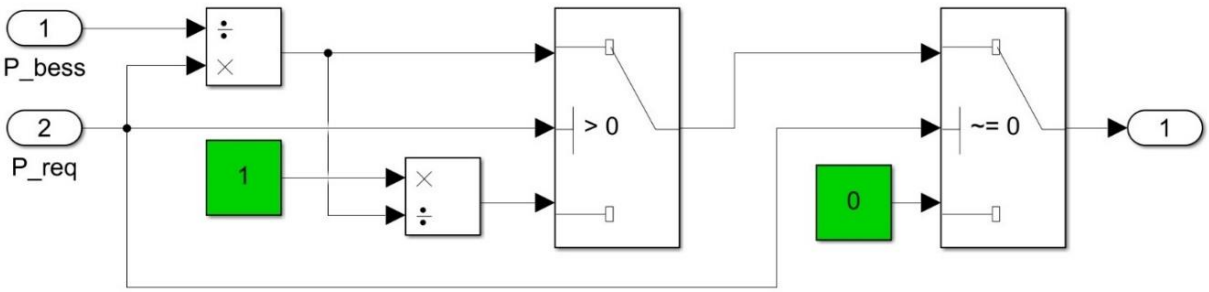

Figure 4.9 Efficiency computation

4.4 Validation

In order to evaluate the proposed model, some validation calculations are needed to be investigated. There are two errors with the name of "SOC estimation error" and "Energy estimation error" that clarify the accuracy of the model in terms of SOC and energy delivery. Additionally, calculation of the energy flow is another important parameter. They are explained in the following:

4.4.1 SOC estimation error

SOC estimation error (e_{SOC}) is defined as the difference between the real SOC (SOC_{real}) after reaching a stationary state (retrieved as a function of OCV using SOC-OCV curve) at the end of the test and SOC estimated by model (SOC_{model}) at the end of the simulation. This term shows the deviation of the estimated final SOC by model from the real battery SOC at the end of the test.

$$e_{SOC} = SOC_{real} - SOC_{model} \quad [\%] \qquad (4.2)$$

4.4.2 Energy estimation error

This term provides a dimensionless figure of the estimation error with respect to the total energy exchanged with the grid within a test. Energy estimation error (e_E) is defined as the ratio between e_{SOC} multiplied by nominal energy (E_{nom}) and the total absolute value of energy flown during verification test, obtained integrating on time the absolute value of power injected or absorbed AC-side.

$$e_{SOC} = \frac{(\frac{e_{SOC} \cdot E_{nom}}{100})}{\int |P_{gridAC}| . dt} . 100 \quad [\%] \tag{4.3}$$

4.4.3 Energy flow

It provides the amount of energy flows, absorbed or injected, through the system during the test. It is defined as the difference between the initial SOC of the battery and its final value at the end of the test, multiplied by the nominal energy of the battery.

$$Energy\ flow = (SOC_{initial} - SOC_{final}) . Enom \quad [MWh] \tag{4.4}$$

Chapter 5

Results

In this study, the model investigated by the real charge/discharge data obtained from an experimental campaign [109]. P_n and E_n are given as initialized parameters of the BESS to the simulation. They are useful in the construction of the control strategy since it is convenient to define the power setpoints as a function of P_n [per unit]. furthermore, the model uses both power setpoints and c-rates. The energy-to-power ratio (EPR) is used to transform from one quantity into the other one.

The overall efficiency is calculated via the BESS efficiency lookup table, and then the SOC is estimated based on the injected or absorbed energy flow by the BESS. The basic assumption here is that the battery operates symmetrical in both charge and discharge cycles so that the η_{BESS} is equal in the charging and discharging cycles.

The model described in chapter 4 is implemented on a workstation with Intel® Core i7-4790 processor, 16 GB of ram, 1 TB hard drive, 64-bit windows 10 pro operating system, and MATLAB Simulink R2019a. This software can simulate the ancillary services provided

to the grid by the BESS, operational efficiency of the BESS, energy flow through the grid, SOC estimation, and power limitations for safe operation of the BESS during all processes.

5.1 Validation of the model

In order to evaluate the developed empirical model, it is compared both with an electrical model, and the real SOC of the battery obtained from the practical experiment. For the tests, three different data sets are used as frequency trends. They are applied to the models to analyze their accuracy in terms of SOC estimation during PCR provision. The initial SOC for each test is different (low, medium, and high SOC). These three different SOC are selected for the test in order to check the behavior of the models with different initial value as SOCs. The results of all tests are provided in the following:

For all tests the nominal power (P_n) and nominal energy (E_n) are considered equal to 1 MW, 2.28 MWh respectively. The nominal frequency of the power system for this work is considered 50Hz. The initial SOC of the battery for low, medium, and high SOC is 24.40%, 52.10%, and 80.95% respectively. The number of samples for the low SOC is 177855, which equals to 49hours and 24minutes. It means that the battery was under the test for 49hours and 24minutes, and the sampling rate was each second. The number of samples for each of the medium and high SOC is 86477, which equals to 24hours. The frequency trend, power setpoint, SOC evolution of the models and the comparison with respect to the SOC retrieved by the SOC-OCV curve at the end of the test (blue stars) are shown in the Figure 5.1, Figure 5.2, Figure 5.3.

5.1.1 Low initial SOC

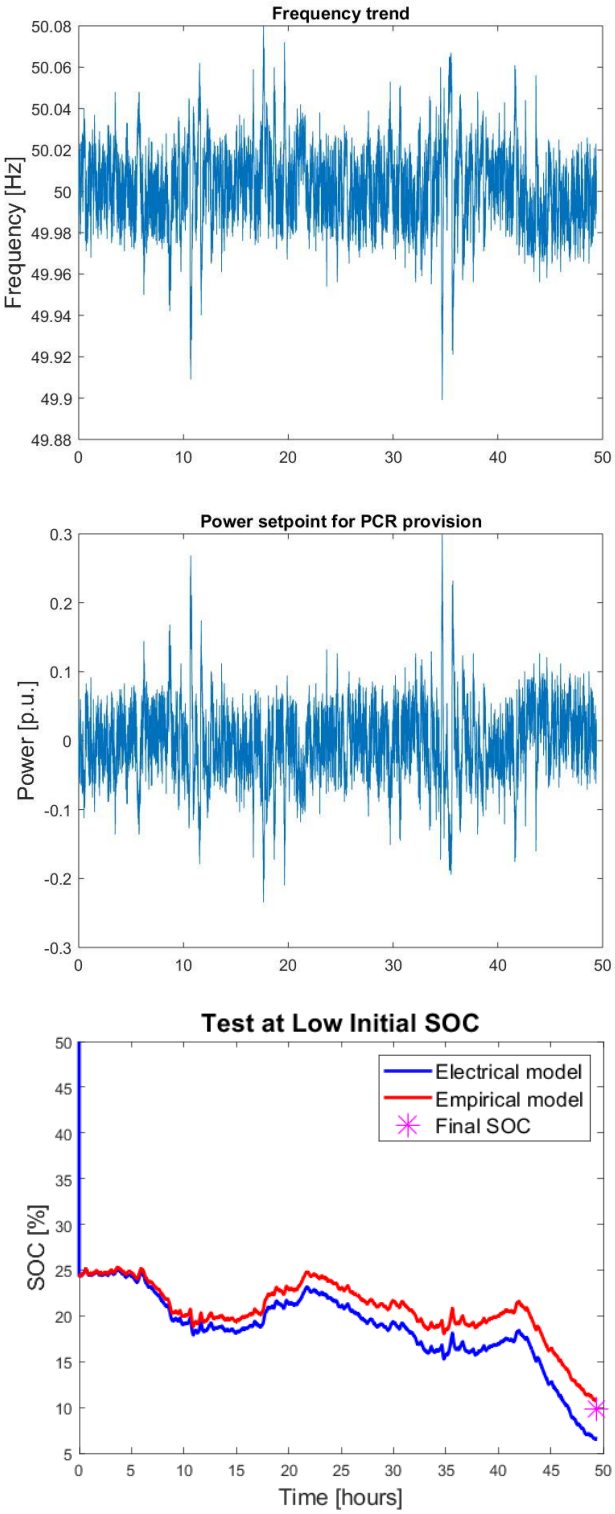

Figure 5.1 Frequency trend, Power setpoint, and SOC estimation with models during PCR

5.1.2 Medium initial SOC

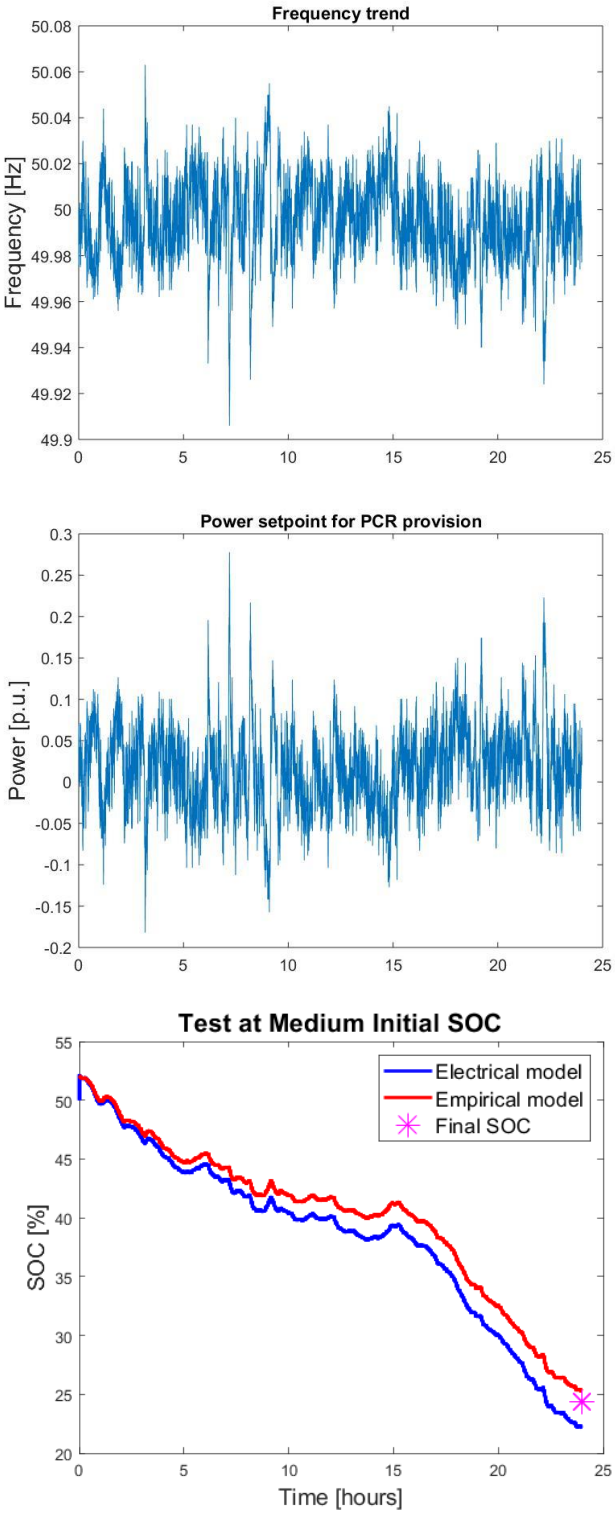

Figure 5.2 Frequency trend, Power setpoint, and SOC estimation with models during PCR

5.1.3 High initial SOC

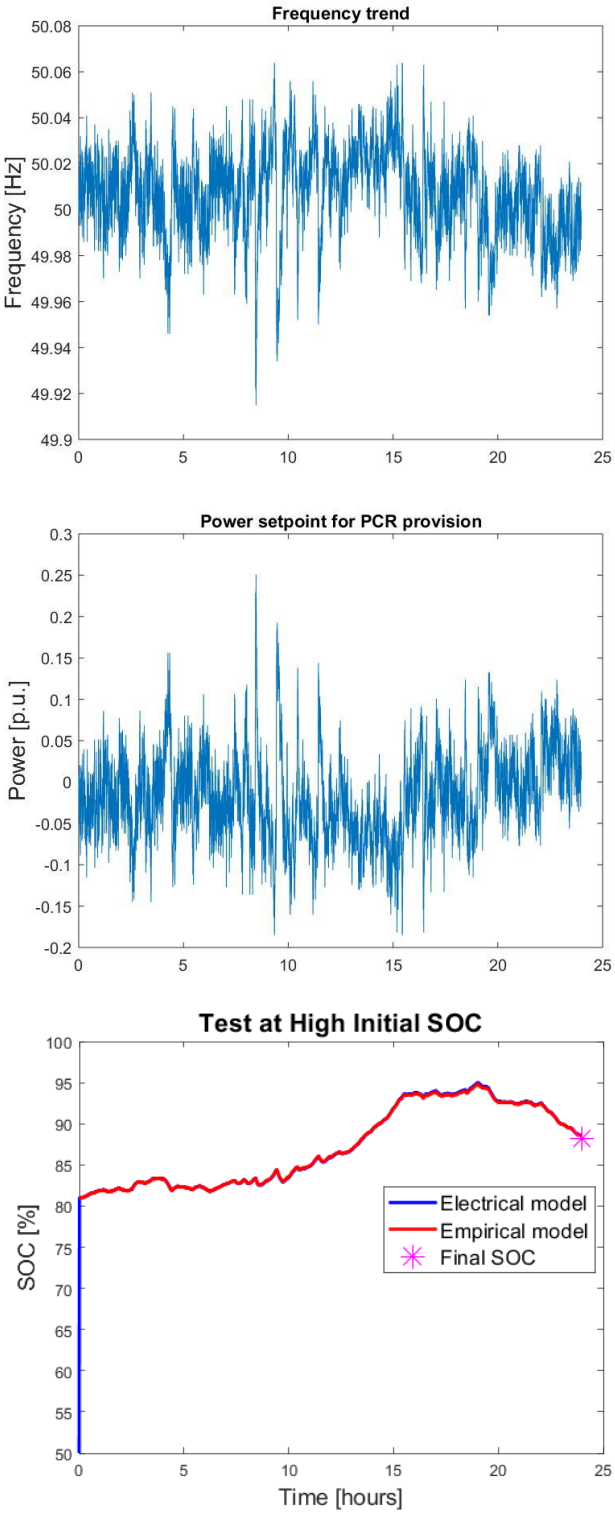

Figure 5.3 Frequency trend, Power setpoint, and SOC estimation with models during PCR

The results of the validation tests for the two models compared with real battery test are shown in Table 5.1, Table 5.2, Table 5.3.

Table 5.1 Result comparison of the three cases for low SOC

Low SOC (24.40%)			
	Electrical model	**Empirical model**	**Real battery**
Elapsed time	≈ 4m 06sec	≈ 23sec	≈ 49h 24m
Estimated Final SOC [%]	6.5735	10.8177	9.80
SOC variation [%]	17.8265	13.5823	14.60
Energy flow [kWh]	406.44	309.67	332.88
Model efficiency [%]	73.35	76.75	---
e_{SOC} [%]	3.2265	-1.0177	0
e_E [%]	22.10	-6.9703	0

As shown in Table 5.1 (Test for Low SOC), the elapsed time for the empirical model is much less than the electrical model. SOC variation term shows that the empirical model has a lower difference between initial SOC and final SOC which causes smaller energy flow. In term of estimated final SOC, the empirical model reaches a closer value to the real battery SOC. Thus, it leads to a lower SOC estimation error (e_{SOC}) in compared to electrical model. Its energy estimation error (e_E) is also lower than the electrical model, because of lower SOC error. The SOC error and energy estimation error are negative for the empirical model because of its higher estimated final SOC than the real battery SOC. Additionally, the overall efficiency of the empirical model is higher than the electrical one. The overall efficiency of both models is limited as the battery was requesting low power for a long time during the tests. This situation is called non-convenient area, in which the efficiency of the PCS (Inverter + Transformer) is lower than when they provide higher power.

Table 5.2 (Test for High SOC) shows the same result in terms of time consumption for the models, but this time electrical model shows a better energy estimation error in compared to the previous test. It still has a higher error value than the empirical model. For this test, the empirical model gets better results in all parameters.

Table 5.2 Result comparison of the three cases for medium SOC

Medium SOC (52.10%)			
	Electrical model	**Empirical model**	**Real battery**
Elapsed time	≈ 1m 58sec	≈ 12sec	≈ 24h 00m
Estimated Final SOC [%]	22.1558	25.2683	24.40
SOC variation [%]	29.94	26.83	27.70
Energy flow [kWh]	682.63	611.72	631.56
Model efficiency [%]	73.63	77.44	---
e_{SOC} [%]	2.24	-0.87	0
e_E [%]	8.08	-3.14	0

Table 5.3 Result comparison of the three cases for high SOC

High SOC (80.95%)			
	Electrical model	**Empirical model**	**Real battery**
Elapsed time	≈ 3m 19sec	≈ 12sec	≈ 24h 00m
Estimated Final SOC [%]	88.55	88.5434	88.25
SOC variation [%]	-7.6	-7.59	-7.3
Energy flow [kWh]	173.28	173.05	166.44
Model efficiency [%]	74.48	74.25	---
e_{SOC} [%]	-0.3	-0.29	0
e_E [%]	-4.11	-3.97	0

Finally, Table 5.3 shows that with increasing the initial SOC, the electrical model becomes more accurate, but even in this case (High SOC) which is not favorable because of its vicinity to the high limitation area, its results are very close to the empirical mode. So, what is the benefit of using electrical model, spending a lot of time for simulation, and finally achieve the same result or worse than the new proposed empirical model?

From the previous tests, it is not exactly clear how these two models are in terms of time consumption. So, it is better to do a test for both periods of 1 day and 1 year. For this test a frequency profile with a duration of 1 year is generated and both models are tested with it. The results verified that the empirical model is almost 10 times faster than the electrical model.

Table 5.4 Evaluation of time consumption for electrical and empirical models.

		Electrical model	**Empirical model**
Elapsed time	1 day	≈ 1m 58sec	≈ 12sec
	1 year	≈ 11h 48min	≈ 1h 13min
Ratio of elapsed time		**9.83**	

Chapter 6

Conclusion

In this work, the feasibility of a Battery Energy Storage System in providing frequency services to the electrical network has been investigated in the framework of the Ancillary Services Market. In particular, this work is focused on single service provision, Primary Control Reserve.

The development, validation, and verification of an empirical Li-ion BESS model based on experimental data. One of the drawbacks for empirical models is the lower accuracy in compared to electrochemical and electrical models, but for providing different services such as PCR, SCR, TCR, and integration with RES in the grid, a high degree of accuracy is inevitable. So, the main goal of this work was to check if it is possible to increase the accuracy of empirical models in terms of SOC estimation. The solution suggested here was to implement an efficiency calculation block based on the real behavior of a Li-ion battery instead of using Polynomial functions. The related characterized data of the battery behavior is extracted from [109].

For the comparison, a passive Electrical model is used. According to the results, the proposed Empirical model not only is 10 times faster than Electrical model, but also has a closer estimated final SOC to the real battery than the electric model. Thus, it has a lower SOC estimation error (e_{SOC}) and energy estimation error (e_E) in compared to electrical model. In addition, the Empirical model has a higher accuracy as well. For all aforementioned reasons, the proposed Empirical model is more robust than the Electrical model. It should be note that the battery was used in a non-convenient area, requesting low power for a long time. Efficiency of the PCS (Inverter + Transformer) is low in that area and limit the overall efficiency of the BESS model.

Some limitations or approximations are accepted in order to provide a procedure applicable by the BESS operator with reasonable timing and effort. As the designing of a new controller was not under the scope of this work, a basic controller with simplified droop curve is used. The reason for the utilization of a droop curve without a dead band was a decrement in the test duration due to the its incrementation in energy flow during the test. So, for future work it is better to develop a new droop curve, and test the model with the new controller.

Appendix

Appendix A: Experimental setup of the BESS

The BESS tested in the experimental campaign is a Li-ion BESS for stationary application present in JRC's Smart Grid and Interoperability Laboratory (SGILab) in Ispra (Italy) [110]. The BESS layout is shown in Figure 6.1.

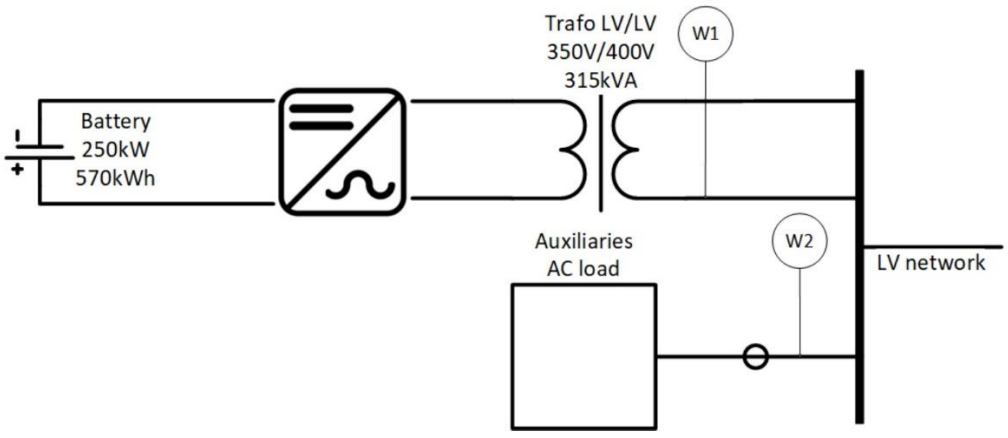

Figure 6.1 BESS scheme with measurement boxes position [109].

A Li-ion nickel-manganese-cobalt (NMC) battery pack of nominal energy (E_n) of 570 kWh and a nominal power (P_n) of 250 kW, whose datasheet is presented in Table 6.1. The system was installed in an external container (Figure 6.2 a) and was made up of 144 battery modules clustered in 12 racks (Figure 6.2 b). The system had a DC-side protection

switchboard. At the end of life (EoL), the BESS is guaranteed for a minimum $E_{n,EoL}$, and $P_{n,EoL}$ of 450 kWh and 225 kW.

Table 6.1 Battery pack essential datasheet [109].

Cell	
Technology	Li-ion
Capacity [Ah]	68
Voltage Range [V]	3.1 to 4.1
Module	
Capacity [kWh]	3.97
Voltage Range [V]	49.6 to 65.5
System	
Design Capacity [kWh]	571.9
Nominal Power [kW]	250
Cells	2304
Modules	144
Racks	12
Minimum Voltage [V]	595.2
Nominal Voltage [V]	700.8
Maximum Voltage [V]	787.2
Nominal Current [A]	357.0

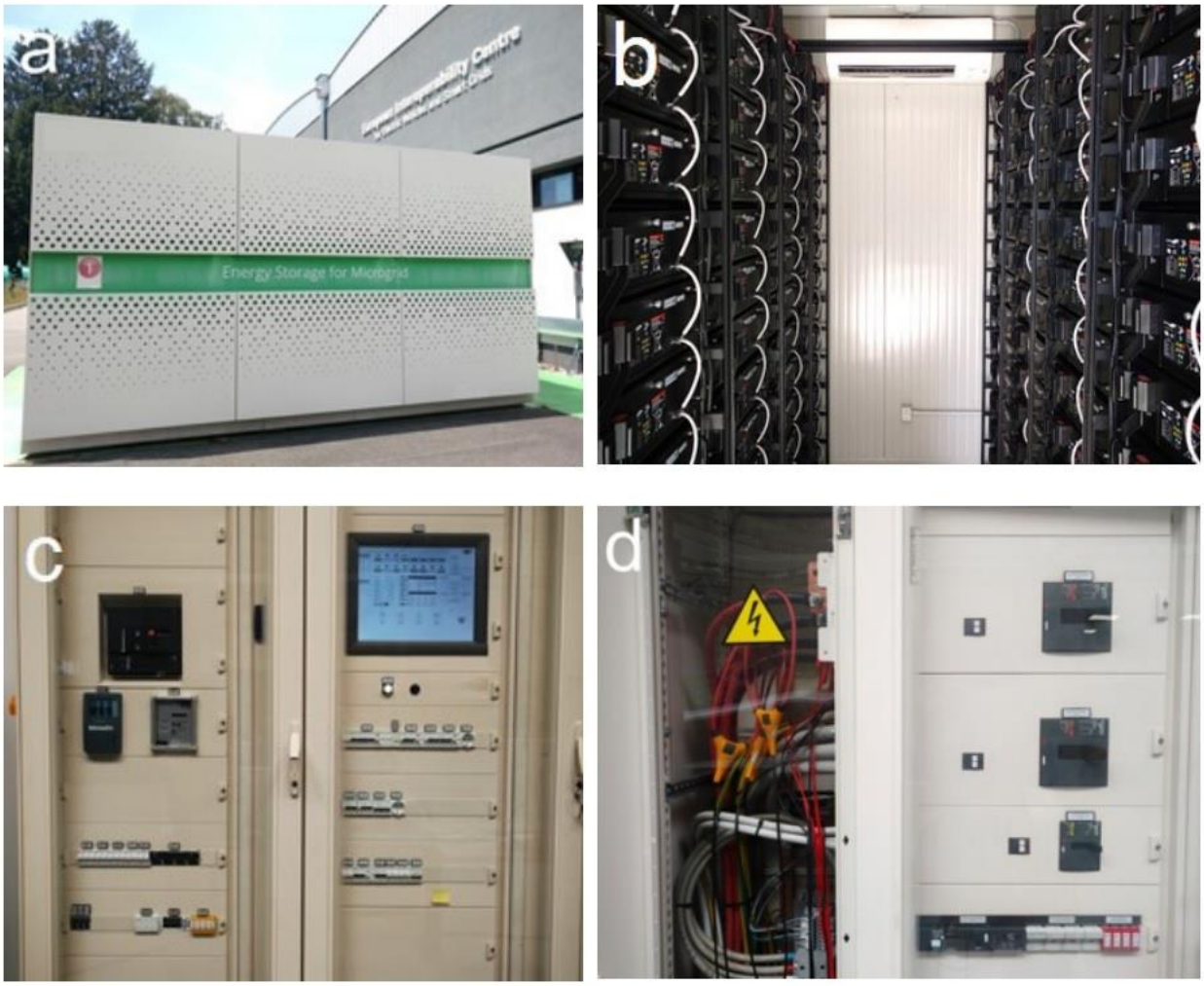

Figure 6.2 The BESS setup: battery container (a), racks (b), SCADA (c), switchboard and feeder (d).

List of Acronyms

AC	Alternate Current
AGC	Automatic Generator Control
AS	Ancillary Services
ASM	Ancillary Services Market
BESS	Battery Energy Storage System
BMS	Battery Management System
BoL	Beginning of Life
DAM	Day-Ahead Market
DB	Dead Band
DER	Distributed Energy Resources
DG	Distributed Generation
DNO	Distribution Network Operators
DoD	Depth of Discharge
DR	Demand Response
EIS	Electrochemical Impedance Spectroscopy
EoL	End of Life

EPR	Energy to Power Ratio
EV	Electric Vehicle
FACTS	Flexible Alternating Current Transmission System
FCR	Frequency Containment Reserves
FERC	Federal Energy Regulatory Commission
FRR	Frequency Restoration Reserves
GME	Gestore Dei Mercati Energetici
HV	High Voltage
ISO	Independent System Operator
Li-ion	Lithium-Ion Battery
LIB	Lithium-Ion Battery
LFC	Load Frequency Control
LUT	Lookup Table
LV	Low Voltage
MV	Medium Voltage
NERC	North America Reliability Council
OCV	Open Circuit Voltage
ORNL	Oak Ridge National Laboratory
PCR	Primary Control Reserve
PDE	Partial Differential Equations
PFR	Primary Frequency Regulation
PV	Photovoltaic
PX	Power Exchange
Reg-Up	Regulation Up
Reg-Down	Regulation Down

RES	Renewable Energy Sources
ROCOF	Rate of Change of Frequency
RPM	Revolution Per Minute
RR	Replacement Reserves
SCR	Secondary Control Reserve
SEI	Solid-Electrolyte Interphase
SFR	Secondary Frequency Regulation
SOA	Safe Operating Area
SoC	State of Charge
SoH	State of Health
TCR	Tertiary Control Reserve
TFR	Tertiary Frequency Regulation
TSO	Transmission System Operator
UPS	Uninterruptible Power Supply

References

[1] IRENA, "Renewable Energy statics 2019," International Renewable Energy, Abu Dhabi, UAE, 2019.

[2] A. Oudalov, R. Cherkaoui, A. Beguin, "Sizing and optimal operation of battery energy storage system for peak shaving application," *In Proc. IEEE Lausanne Power Tech*, p. 621–625, Lausanne, Switzerland, 2007.

[3] B. Belvedere, "A microcontroller-based power management system for standalone microgrids with hybrid power supply," *IEEE Trans. Sustain. Energy*, vol. 3, no. 3, p. 422–431, Jul. 2012.

[4] F. Sossan, E. Namor, R. Cherkaoui and Paolone, "Achieving the dispatchability of distribution feeders through prosumers data driven forecasting and model predictive control of electrochemical storage," *IEEE Trans. Sustain. Energy*, vol. 7, no. 4, p. 1762–1777, Oct. 2016.

[5] X. Ke, N. Lu and C. Jin, "Control and size energy storage systems for managing energy imbalance of variable generation resources," *IEEE Trans. Sustain. Energy*, vol. 6, no. 1, p. 70–78, Jan. 2015.

[6] P. Iurilli, C. Brivio and M. Merlo, "SoC management strategies in Battery Energy Storage System providing Primary Control Reserve," *Sustainable Energy, Grids and Networks*, Vols. 19, 100230, Sep. 2019.

[7] K. Christakou, D.-C. Tomozei, M. Bahramipanah, J. Y. L. Boudec and M. Paolone, "Primary voltage control in active distribution networks via broadcast signals: The case of distributed storage," *IEEE Trans. Smart Grid*, vol. 5, no. 5, p. 2314–2325, Sep. 2014.

[8] A. Oudalov, D. Chartouni and O. C., "Optimizing a battery energy storage system for primary frequency control," *IEEE Trans. Power Syst.,* vol. 22, no. 3, p. 1259–1266, Aug. 2007.

[9] IRENA, "Electricity Storage and Renewables: Costs and Markets to 2030," International Renewable Energy Agency, Abu Dhabi, UAE, 2017.

[10] D. G. AS, "Energy transition outlook 2017, RENEWABLES, POWER AND ENERGY USE FORECAST TO 2050," 2017. [Online]. Available: https://www.dnvgl.com.

[11] IEA, "Global EV Outlook," International Energy Agency, Paris, France, 2019, pg. XX.

[12] "ElectronicsToturials," [Online]. Available: https://www.electronics-tutorials.ws/capacitor/ultracapacitors.html.

[13] "Better World Solution," Smart Grid Energy Storge: Flywheels, [Online]. Available: https://www.betterworldsolutions.eu/smart-grid-energy-storage-flywheels/.

[14] "storage, Flywheel energy, wikipedia," [Online]. Available: https://en.wikipedia.org/wiki/Flywheel_energy_storage#NASA_G2_flywheel_for_spacecraft_energy_storage.

[15] J. Stewart, Flywheels move from steam age technology to Formula 1, 2012.

[16] "Breakthrough in Ricardo Kinergy 'second generation' high-speed flywheel technology Press r," Ricardo, 2011. [Online]. Available: https://ricardo.com/news-and-media/news-and-press/breakthrough-in-ricardo-kinergy-%e2%80%98second-generation.

[17] "10 Need-to-Know Tech Concepts for 2012," popularmechanics, Jan 2012. [Online]. Available: popularmechanics.com.

[18] FCHEA, "Fuel Cell & Hydrogen Energy Association," 2018. [Online]. Available: http://www.fchea.org/fuelcells.

[19] T. P. J. Crompton, Battery Reference Book 3rd edition, ISBN: 9780080499956, London: Elsevier, 2000.

[20] G. Pistoia, Batteries for Portable Devices , ISBN 978-0-08-045556-3, Elsevier, 2016.

[21] Energizer, "Alkaline Manganese Dioxide Handbook and Application Manual," Energizer, 2008.

[22] "Electrolytes, Zeta Potential Analysis of Lithium Ion Battery; AZOM," AZO Material, 2017. [Online]. Available: https://www.azom.com/article.aspx?ArticleID=14584.

[23] "Speedy tech," 2019. [Online]. Available: https://bdspeedytech.com/index.php?route=product/product&product_id=2475.

[24] M. S. Ballon, "Electrovaya, Tata Motors to make electric Indica," 14 Oct 2008. [Online]. Available: www.cleantech.com.

[25] Encyclopædia Britannica, Inc., [Online]. Available: https://www.britannica.com/technology/storage-battery.

[26] Battery mart, [Online]. Available: https://www.batterymart.com/p-aa-700-sanyo-consumer-top-nicd-battery.html.

[27] N.-b. Batteries, "Battery University," 25 02 2020. [Online]. Available: https://batteryuniversity.com/learn/article/nickel_based_batteries.

[28] P. Kurzweil and J. Garche, "Overview of batteries for future automobiles," in *Lead-Acid Batteries for Future Automobiles*, Elsevier, 2017, pp. 27-96.

[29] K. Chau, Y. Wong and C. Chan, "An overview of energy sources for electric vehicles," *Energy Conversion and Management*, vol. 40, pp. 1021-1039, 1999.

[30] W. paper, "Electrical Energy Storage.," in *The International Electrotechnical Commission (IEC)*, Geneva, Switzerland, 2011.

[31] "lindinger," [Online]. Available: https://www.lindinger.at/en/batteries/lead-batteries/multipower-lead-acid-battery-mp12-12c-pb-12v-12a-h.

[32] D. Linden and T. Reddy, Handbook of batteries, 3rd ed., New York: McGraw-Hill, Inc, 2001.

[33] S. Lukic, J. Cao, R. Bansal, F. Rodriguez and A. Emadi, "Energy storage systems for automotive applications," *IEEE Trans Ind Electron,* vol. 55, no. 6, p. 2258–2267, 2008.

[34] M. Rashid, Power electronics handbook, 3rd ed., USA: Butterworth-Heinemann publications, 2011.

[35] lead_based_batteries, "Battery University," 2019. [Online]. Available: https://batteryuniversity.com/learn/article/lead_based_batteries.

[36] I. Bloom and e. al., "An accelerated calendar and cycle life study of Li-ion cells," *Journal of Power Sources,* vol. 101, no. 2, 2001.

[37] B. Stiaszny, J. C. Ziegler, E. E. Krauß, M. Zhang, J. P. Schmidt and E. Ivers-Tiffée, "Electrochemical characterization and post-mortem analysis of aged LiMn2O4 NMC/graphite lithium ion batteries part II: Calendar aging," *Journal of Power Science,* vol. 258, pp. 61-75, 2014.

[38] M. B. Pinson and M. Z. Bazant, "Theory of SEI formation in Rechargeable Batteries: Capacity fade, accelerated ageing and lifetime prediction," 2012.

[39] J. Vettera, P. W. M. Nováka, C. Veitb, K.-C. Möller, J. Besenhard, M. Winter, M. Wohlfahrt-Mehrensc, C. Vogler and A. Hammouched, "Ageing mechanisms in lithium-ion batteries," *Journal of Power Sources,* vol. 147, no. 1–2, pp. 269-281, 9 September 2005.

[40] M. Takahashi, S. I. Tobishima, K. Takei and Y. Sakurai, "Reaction behavior of LiFePO4 as a cathode material for rechargeable lithium batteries," , vol. , nos. 3/4, pp. 283–289, Jun," *Solid State Ion,* vol. 148, no. 3/4, p. 283–289, Jun. 2002.

[41] S. Lee, H. Cui, M. Rezvanizaniani and J. Ni, "Battery prognostics: SoC and SoH prediction," *in Proc. ASME Int. Manuf. Sci. Eng. Conf. (MSEC), Notre Dame, IN, USA,* p. 689–695, Jun. 2012.

[42] B. Yang, Z. Chen, J. Xue, Q. Xu, J. Sun, Y. Xiao and Z. Liu, "Experimental temperature variation in battery pack with unbalanced SOCs during charging process," in *13th IEEE Conference on Industrial Electronics and Applications (ICIEA),* Wuhan, June. 2018.

[43] C. K. Park, Z. W. Zhang, Z. Q. Xu, A. Kakirde, K. Kang, C. Chai, G. Au and L. Cristo, "Variables study for the fast charging lithium ion batteries," *JOURNAL OF POWER SOURCES,* vol. 165, pp. 892-896, 2007.

[44] A. S. Andersson and J. O. Thomas, "The source of first-cycle capacity loss in LiFePO4," *JOURNAL OF POWER SOURCES*, vol. 97, no. 8, pp. 498-502, 2001.

[45] Team, "A Guide to Understanding Battery Specifications," MIT Electric Vehicle, Dec. 2008.

[46] G. Rancilio, "Battery Energy Storage Systems for Ancillary Services Provision," 2018.

[47] D. V. Ragone, "Review of Battery Systems for Electrically Powered Vehicles," *SAE Technical Paper. doi:10.4271/680453. 680453,* 1968.

[48] T. Christen and M. W. Carlen, "Theory of Ragone plots," *Journal of Power Sources,* vol. 91, no. 2, p. 210–216, 2000.

[49] S. C. Lee and Y. J. Woo, "Analogical understanding of the Ragone plot and a new categorization of energy device," *Energy Procedia,* vol. 88, p. 526–530, 2016.

[50] I. S. Jacobs and C. P. Bean, "Fine particles, thin films and exchange anisotropy," *in Magnetism,* Vols. 3, G. T. Rado and H. Suhl, Eds. NewYork, NY, USA, p. 271–350, 1963.

[51] M. A. Hannan, M. S. H. Lipu, A. Hussain and A. Mohamed, "A review of lithium-ion battery state of charge estimation and management system in electric vehicle applications: Challenges and recommendations," *Renew. Sustain. Energy Rev,* vol. 78, p. 834–8, Oct. 2017.

[52] K. Ng, C.-S. Moo, Y.-P. Chen and Y.-C. Hsieh, "Enhanced coulomb counting method for estimating stateof-charge and state-of-health of lithium-ion batteries," *Appl. Energy,* vol. 86, pp. 1506–1511, doi:10.1016/j.apenergy.2008.11.021, 2009.

[53] L. Zhao, M. Lin and Y. Chen, "Least-squares based coulomb counting method and its application for state-ofcharge (soc) estimation in electric vehicles. 2016, 40,," *Int. J. Energy Res.,* vol. 40, pp. 1389–1399, doi:10.1002/er.3530, 2016.

[54] Q.-K. Wang, Y.-J. He, J.-N. Shen, X.-S. Hu and Z.-F. Ma, "State of Charge-Dependent Polynomial Equivalent Circuit Modeling for Electrochemical Impedance Spectroscopy of Lithium-Ion Batteries," *IEEE TRANSACTIONS ON POWER ELECTRONICS,* vol. 33, no. 10, Oct. 2018.

[55] Y. MA, X. LI, G. LI, Y. HU and Q. BAI, "SOC Oriented Electrochemical-Thermal Coupled Modeling for Lithium-Ion Battery," *IEEE ACCESS,* Nov. 2019, Doi: 10.1109/ACCESS.2019.2949357.

[56] W. He, M. Pecht, D. Flynn and F. Dinmohammadi, "A Physics-Based Electrochemical Model for LithiumIon Battery State-of-Charge Estimation Solved by an Optimised Projection-Based Method and MovingWindow Filtering," *MDPI, Energies,* Aug. 2018.

[57] Y. Xing, W. He, M. Pecht and K. Tsui, "State of charge estimation of lithium-ion batteries using the opencircuit voltage at various ambient temperatures," *Appl. Energy* , vol. 113, pp. 106–115, doi:10.1016/j.apenergy.2013.07.008, 2014.

[58] T. Feng, L. Yang, X. Zhao, H. Zhang and J. Qiang, "Online identification of lithium-ion battery parameters based on an improved equivalent-circuit model and its implementation on battery state-of-power prediction. J.," *Power Sources* , vol. 281, pp. 192–203, doi:10.1016/j.jpowsour.2015.01.154, 2015.

[59] F. Sun, R. Xiong and H. He, "A systematic state-of-charge estimation framework for multi-cell battery pack in electric vehicles using bias correction technique," *Appl. Energy,* vol. 162, p. 1399–1409, 2016.

[60] A. Vezzini, "15-Lithium-Ion Battery Management.," *In Lithium-Ion Batteries, Elsevier,* p. 345–360, 2014.

[61] C. Y. o. Chun, J. Baek, G.-S. Seo, B. Cho, J. Kim, I. K. Chang and S. Lee, "Current sensor-less state-of-charge estimation algorithm for lithium-ion batteries utilizing filtered terminal voltage," *Journal of Power Sources,* vol. 27, no. 1, pp. 255-263, Jan. 2015.

[62] L. Gao, S. Liu and R. A. Dougal, "Dynamic lithium-ion battery model for system simulation," *IEEE Trans. Component Package Technology,* vol. 25, no. 3, pp. 495-505, Sep.2002.

[63] M. Brenna, F. Foiadelli, M. Longo, S. Barcellona and L. Piegari, "Lithium-ion battery: A simplified modeling procedure and system simulation," *International Symposium on Power Electronics, Electrical Drives, Automation and Motion, SPEEDAM,* pp. 1034-1040, 2016.

[64] S. Barcellona and L. Piegari, "A lithium-ion capacitor model working on a wide temperature range," *Journal of Power Sources,* vol. 342, pp. 241-251, Feb. 2017.

[65] J. Li and M. S. Mazzola, "Accurate battery pack modeling for automotive applications," *Journal of Power Sources*, vol. 237, pp. 215-228, 2013.

[66] S. Castano, L. Gauchia, E. Voncila and J. Sanz, "Dynamical modeling procedure of a Li-ion battery pack suitable for real-time," *Energy Conversion and Management*, vol. 92, pp. 396-405, Mar. 2015.

[67] A. Shafiei, A. Momeni and S. Williamson, "Plug-in hybrid electric vehicle charging: Current issues and future challenges," in *Vehicle Power and Propulsion Conference (VPPC)*, 2011, pp. 1-5.

[68] C. Sen, S. Member, N. Kar and S. Member, "IEEE Vehicle Power and Propulsion Conference (VPPC)," in *IEEE*, Michigan, 2009, pp. 207-212..

[69] R. Kroeze and P. Krein, "IEEE Power Electronics Specialists Conference," in *IEEE*, 2008, pp. 1336-1342.

[70] J. Kim, J. Shin, C. Chun and B. Cho, *IEEE Transactions on Power Electronics*, vol. 27, pp. 411-424, 2012.

[71] M. Dubarry, N. Vuillaume and B. Liaw, "From single cell model to battery pack simulation for Li-ion batteries," *Journal of Power Sources 186*, vol. 186, pp. 500-507, 2009.

[72] N. Watrin, D. Bouquain, B. Blunier and A. Miraoui, "Multiphysical lithium-based battery pack modeling for simulation purposes," in *IEEE Vehicle Power and Propulsion Conference* , 2011.

[73] R. Carter, A. Cruden, P. Hall and A.S. Zaher, *IEEE Transactions on Energy Conversion*, vol. 27, p. 2012, 21-28.

[74] S. Lajeunesse, in *Twenty-Seventh Annual IEEE Applied Power Electronics Conference and Exposition (Apec)*, Coronado Springs in Disneyworld, Orlando, Florida, Feb. 2012.

[75] Y. Chen, X. Liu, Y. Cui, J. Zou and S. Yang, "A MultiWinding Transformer Cell-to-Cell Active Equalization Method for Lithium-Ion Batteries With Reduced Number of Driving Circuits," *IEEE Transactions on Power Electronics*, vol. 31, no. 07, pp. 4916-4929 , 2016.

[76] M. Liu, M. Fu, Y. Wang and C. Ma, "Battery Cell Equalization via Megahertz Multiple-Receiver Wireless Power Transfer," *IEEE Transactions on Power Electronics,* vol. 33, no. 5, pp. 4135-4144, Jun. 2017.

[77] A. D. Papalexopoulos, "Design of an Efficient Ancillary Services Market," in *IEEE Power Engineering Society General Meeting*, Tampa, FL, USA, 2007.

[78] K. Counsell and L. Evans, "Day-Ahead Electricity Markets: Is There a Place for a DayAhead Market in the NZEM?," New Zealand Institute for the study of Competition and Regulation Inc., 2003.

[79] G. d. M. E. GME, "Mercato elettrico a pronti (MPE)," [Online]. Available: [Online]. Available: http://www.mercatoelettrico.org/it/Mercati/MercatoElettrico/MPE.aspx..

[80] O. KILNYTSKYI, "Electricity Market Reform: How Large Consumers Can Avoid Losses. An Algorithm of Actions," Mind, Nov. 2018. [Online]. Available: https://mind.ua/en/publications/20191031-electricity-market-reform-how-large-consumers-can-avoid-losses-an-algorithm-of-actions.

[81] M. e. al, Market Operation in Electric Power System, John Wily, 2002.

[82] "commission, Federal Energy Regulatory," 2005. [Online]. Available: http://WWW.ferc.gov.

[83] "Laboratory, Oak Ridge National," 2004. [Online]. Available: http://www.nerc.com.

[84] J. T. Alt, M. D. Anderson and R. G. Jungst, "Assessment of Utility Side Cost Savings from Battery Energy Storage," *IEEE Transactions on Power Systems,* 1997.

[85] O. A. a. C. Daniel, "Optimizing a Battery Energy Storage System for Primary Frequency Control," *IEEE Transactions on Power Systems,* 2007.

[86] S. Cho, "Operation of Battery Energy Storage System for Governor Free and its Effect," *The Transactions of the Korean Institute of Electrical Engineers,* 2015.

[87] F. Gonzalez-Longatt, E. Chikuni and E. Rashayi, "Effects of the Synthetic Inertia from Wind Power on the Total System Inertia after a Frequency Disturbance".

[88] H. Jo, J. Choi and K. A. Agyeman, "Development of frequency control performance evaluation criteria of BESS for ancillary service: A case study of frequency regulation by KEPCO," in *IEEE Innovative Smart Grid Technologies - Asia (ISGT-Asia)*, Auckland, New Zealand, 2018.

[89] ABB, "Energy storage-keeping smart grids in balance," in *ABB Energy Storage*, 2012.

[90] J. Schmutz, "Primary frequency control provided by battery," in *EEH Power Systems Laboratory*, Zurich, 2013.

[91] S.-A. Amamra, B. Francois and J. Lugaro, "Day-ahead primary power reserve planning and day-D primary frequency control of a Li-ion battery," in *2015 IEEE Eindhoven PowerTech*, Eindhoven, 2015.

[92] A. M. Ersdal, L. Imsland, K. Uhlen, D. Fabozzi and N. F. Thornhill, "Model Predictive Load-Frequency Control Taking into Account Imbalance Uncertainty," in *Control Engineering Practice*, 2015.

[93] Terna, "Allegato A.15 - Partecipazione alla regolazione di frequenza e frequenza/potenza", Codice di Rete," 2008.

[94] T.-S. A. Pubblica, "Livelli Regolazione Secondaria," Online.

[95] N. Vovos, A. E. Kirprakis, A. R. Wallace and G. P. Harrison., "Centralised and distributed voltage control: Impact on distributed generation penetration," *IEEE Trans. on Power Systems*, vol. 22, no. 1, p. 476–482, Feb. 2007.

[96] P. Harrison and A. R. Wallace, "Maximising renewable energy intergartion within electrical networks," in *World Renewable Energy Congress (WREC2005)*, May 2005.

[97] Y. LIU, R. FAN and V. TERZIJA, " Power system restoration: a literature review from 2006 to 2016," *Journal of Modern Power Systems and Clean Energy*, vol. 4, p. 332–341, 2016.

[98] A. Massound, "A smart self-healing grid: in pursuit of a more reliable and resilient system," *IEEE Power Energy Mag*, vol. 12, no. 1, p. 108–112, 2014.

[99] L. YT, W. HT and Y. H, "Power system restoration theory and technology," in *Science and Technology Press*, Beijing, 2014.

[100] Statnett, "Systemdrifts- og markedsutviklingsplan 2012. Tech. rep.," 2012.

[101] J. Short, D. Infield and L. Freris, "Stabilization of grid frequency through dynamic demand control," *IEEE Transactions on Power Systems* , vol. 22, no. 3, p. 1284–1293, Aug. 2007.

[102] F. D., N. F. Thornhill and B. C. Pal, "Frequency restoration reserve control scheme with participation of industrial loads.," in *IEEE Grenoble PowerTech conf*, Grenoble, 2013.

[103] G. Suvire, M. Molina and P. Mercado, "Improving the integration of wind power generation into ac microgrids using flywheel energy storage.," *IEEE Transactions on Smart Grid,* vol. 3, no. 4, p. 1945–1954, Dec. 2012.

[104] G. Delille, "Dynamic frequency control support: A virtual inertia provided by distributed energy storage to isolated power systems," in *ISGT Europe*, 2010.

[105] D. Whitley and O. Gjerde, "Exchange of balancing services between the Nordic and the Central European synchronous systems.," in *LFC/AGC-Nordic and European perspective*, 2011.

[106] Nordel, "Nordel Annual Statistics 1997-2008," 2013.

[107] C. D. Marco, "Primary and secondary control for high penetration renewables," in *Power Systems Engineering Research Centre*, 2012.

[108] V. Ramadesigana, P. Northropa, S. Dea, S. Santhanagopalanb, R. Braatzc and V. Subramaniana, "Modeling and Simulation of Lithium-Ion Batteries from a Systems Engineering Perspective," *J. Electrochem. Soc.*, vol. 159, p. 31–45, 2012.

[109] G. Rancilio, L. Alexandre, K. Evangelos, F. Gianluca, M. Merlo, M. Delfanti and M. Masera, "Modeling a Large-Scale Battery Energy Storage System for Power Grid Application Analysis," *Energies,* 2019.

[110] E. Kotsakis, A. Lucas, N. Andreadou, G. Fulli and M. Masera, "Recent research conducted at the SGILab towards an efficient and interoperable smart grid.," in *Proceedings of the AEIT International Annual Conference* , Bari, Italy, Oct. 2018.